EFFECT OF FLUID FLOW ON ZINC ELECTRODEPOSITS FROM ACID CHLORIDE ELECTROLYTES

by

ANTOINE ANWAR ABDELMASSIH

SUBMITTED TO THE DEPARTMENT OF
MATERIALS SCIENCE AND ENGINEERING
IN PARTIAL FULFILLMENT OF THE
REQUIREMENTS FOR THE DEGREE OF

MASTER OF SCIENCE

at the

MASSACHUSETTS INSTITUTE OF TECHNOLOGY
February 1982

Signature of author A. AbdelMassih

Department of Materials Science and Engineering
January 14, 1982

Certified by Donald R. Sadoway

Donald R. Sadoway
Thesis Supervisor

Accepted by Régis Pelloux

Régis M.N. Pelloux
Chairman, Departmental Graduate Committee

TABLE OF CONTENTS

LIST OF FIGURES

EFFECT OF FLUID FLOW ON ZINC ELECTRODEPOSITS FROM ACID CHLORIDE ELECTROLYTES

by

ANTOINE ANWAR ABDELMASSIH

Submitted to the Department of Materials Science and Engineering
on January 14, 1982 in partial fulfillment of the
requirements for the Degree of Master of Science in
Materials Engineering

ABSTRACT

Zinc was deposited potentiostatically from acid chloride baths. Once bath chemistry and electrochemistry were controlled, the study was focused on convective mass transfer at horizontal electrodes and its effect on cell performance. A laser schlieren imaging technique allowed in-situ observations of flow patterns and their correlation with current transients.

Convection was turbulent and mass transfer as a function of Rayleigh number was well correlated by :

$$Sh = 0.14\ Ra^{1/3}$$

Similarly, convection initiation time was correlated by

$$\frac{Dt}{d^2} = 38\ Ra^{-2/3}$$

Time scale of fluctuations was about half the initiation time. Taking the boundary layer thickness as a characteristic length, a critical Rayleigh number for the onset of convection was deduced :

$$Ra_{Cr} = 5000$$

Placing the anode on the top of the cathode completely changed the flow pattern but kept the I-t curves identical whereas the use of a cathode grid doubled the limiting current. A well defined plateau in the current-voltage curves suggested that hydrogen evolution has been successfully inhibited. Finally, long time deposition showed that convection at horizontal electrodes increased the induction time for dentrite growth by at least a factor of 2 with respect to a vertical wire.

Thesis Supervisor : Pr. Donald R. Sadoway

Title : Assistant Professor of Materials Engineering

ACKNOWLEDGEMENT

I thank MIT for awarding me a research assistantship. I am specially in debt to Pr. D. R. SADOWAY for the valuable discussions we had together and his constant support. I thank also the technicians in the department of Materials Science and Engineering for the help they provided me.

This work was funded by NASA under contract n° NSG-7645.

INTRODUCTION

Molten salt cells have very interesting properties : high conductivity, high possible current densities etc... However serious problems still limit their applications. One of them is deposit quality. Indeed molten salts electrodeposits are typically incoherent and powdery. The few metals recovered from molten salts are produced in the liquid phase thus avoiding the problem of deposit morphology.

If one can understand the reason for the poor quality of those deposits one may expect to improve it. There would be no need to work above the metal melting temperature and the efficiency of present cells would be considerably increased. Furthermore this would open new perspectives for molten salt electrochemistry in applications as corrosion resistant coatings etc...

The effect of conventional process variables on deposit quality has been extensively studied in the case of aqueous solutions. The importance of the usual parameters, i.e., overvoltage, current density,

concentration, temperature was soon recognized. Certain organic or inorganic substances were found to be good levelling or brightening agents. However mass transport, which has been overlooked for a long time, turned out to be the controlling factor.

It is believed that mass transport is also the key factor in deposition from molten salts and differences in quality of deposits from molten salts and aqueous solutions are due to differences in mass transport properties.

The present work is the first part of a comparative study of deposition from both electrolytes in order to determine those differences. It was focused on the effect of convection and electrode arrangement on mass transfer and cell efficiency. Along with it, was the goal of developping a technique allowing in-situ observations of flow patterns and their correlation with the usual electrochemical variables. Deposition was carried out potentionstaticaly in a transparent cell and flow visualization was possible through a laser schlieren imaging technique.

The test system had to fulfill several conditions :

- The laser schlieren technique requires transparent baths both in aqueous and molten salt solutions so that the laser beam can go through the cell (this rules out metals having coloured aqueous salt such as Fe, Ni, Co, Cu).

- The metal should be in the solid state at temperature above the melting temperature of the ionic electrolyte.

- All the metal ions present in the molten salt should have the same valency (this rules out Al and group IV.b and V.b metals).

- In aqueous solutions at reasonable overpotentials, the metal rather than hydrogen should be deposited (this rules out low hydrogen overpotential metals).

- The metals should be stable in water (this rules out alkali and earth-alkali metals).

In addition it was desirable to have :

- The same anion in both electrolytes.

- Electrochemical data already available in the litterature.

- Easy supply of the metal.

Very few systems fulfill all these requirements. Zinc in acid-chloride baths and KCl-LiCl eutectic melt was finally selected.

In this work, results concerning deposition of zinc from chloride solutions are presented. However, in order to isolate the role of mass transfer in the deposition process, preliminary studies were necessary for a minimum understanding of the chemistry of zinc chloride and the electrochemistry of zinc deposition.

Part one deals with the hydrolysis of zinc chloride. Indeed aqueous

zinc chloride has very unusual properties. It is a fairly strong acid with a trend to self-complexation. At high concentration, there is even evidence of polymerization. Equilibrium calculations and titration measurements allowed a rational selection of compositions and pH values for the solutions used in further experiments. Part two reviews briefly the work done on zinc electrodeposition and electrochemistry. With the insight of the previous section, many of the contradictions reported in the litterature will be explained in terms of differences in bath chemistry. The critical overpotential for dentrite growth from acid chloride solutions was also determined. Finally,part three covers the study of convection and its dependence on overpotential, concentration and cell geometry.

PART I : $ZnCl_2$ AQUEOUS CHEMISTRY

I.1 - $ZnCl_2$ an unusual salt

Group II.b halides exhibit very peculiar properties in aqueous solutions. Those pecularities are well illustrated in the case of $ZnCl_2$ and can be summarized as follows :

- A great affinity to water reflected by a strong hygroscopy, an unusual solubility and a fairly strong acidity.

- A trend towards self-complexation and polymerization with its corresponding effects on transport properties (conductivity, diffusion, transport numbers, viscosity, etc...).

Both features raised the interest of several investigators in the late fifties and early sixties. Many chemists tried to elucidate the first one[1-3] whereas the second was an ideal test for more recent theories on irreversible thermodynamics[4-6]. A variety of techniques were used : from Raman spectroscopy to emf and viscosity measurements including titration experiments and so on. The results can be summarized as follows :

- As much as 32 moles of $ZnCl_2$ can be dissolved in one liter of water (at room temperature)[7].

- Its apparent acidity increases with concentration[2].

- Depending on pH and concentration, low solubility oxychlorides may be present and precipitate as a diffuse gelly substance[6].

- Evidence of chloride complexes exists at concentrations as low as 0.01 M [2-6] and Raman spectroscopy reveals the presence of $ZnCl_4^{2-}$ around 1 M [8].

- At higher concentrations (above 10 M), a polymeric compound is

formed[9]. Correspondingly, a sharp rise in viscosity (several orders of magnitude) is observed.

- Negative transport numbers are reported at concentrations above 2 M [4].

A complete understanding of such a complex chemistry is beyond the scope of this work. However it was necessary to select composition ranges and pH values so that zinc is present in the solution as a single dominant ionic species. Otherwise the system would have been ill-defined and some ambiguity would have pertained regarding any further result. Additional investigations were consequently carried out :

1) Equilibrium calculations were done based on data from Ref.6,8 . It was possible to follow the composition of the solution as the concentration of $ZnCl_2$ is increased. The shift in equilibria, as more chloride ions are added, was also examined.

2) Titration measurements helped to characterize the acidic behavior of $ZnCl_2$ at low pH values.

I.2 - Equilibrium calculations

In aqueous solutions, zinc ions interact with chloride ions and form chloride complexes. The presence of Zn^{2+}, $ZnCl^+$, $ZnCl_2$, $ZnCl_4^{2-}$ ions has been reported independently by several authors[2, 8, 9]. It was possible to obtain even the dissociation constants of those complexes.

$$ZnCl^+ \rightleftharpoons Zn^{2+} + Cl^- \qquad \hat{k} = \frac{a_{Zn^{2+}} \times a_{Cl^-}}{a_{ZnCl^+}} = .22 \ [6] \qquad (1)$$

$$ZnCl_2 \rightleftharpoons Zn^{2+} + 2Cl^- \qquad K_1 = [Zn^{2+}][Cl^-]^2[ZnCl_2]^{-1} = .0315\ M^2 \ [8] \qquad (2)$$

$$ZnCl_4^{2-} \rightleftharpoons ZnCl_2 + 2Cl^- \qquad K_2 = [ZnCl_2][Cl^-]^2[ZnCl_4^{2-}]^{-1} = .04\ M^2 \ [8] \qquad (3)$$

where (2) and (3) are valid only around $[ZnCl_2]_{total} = 2$ M

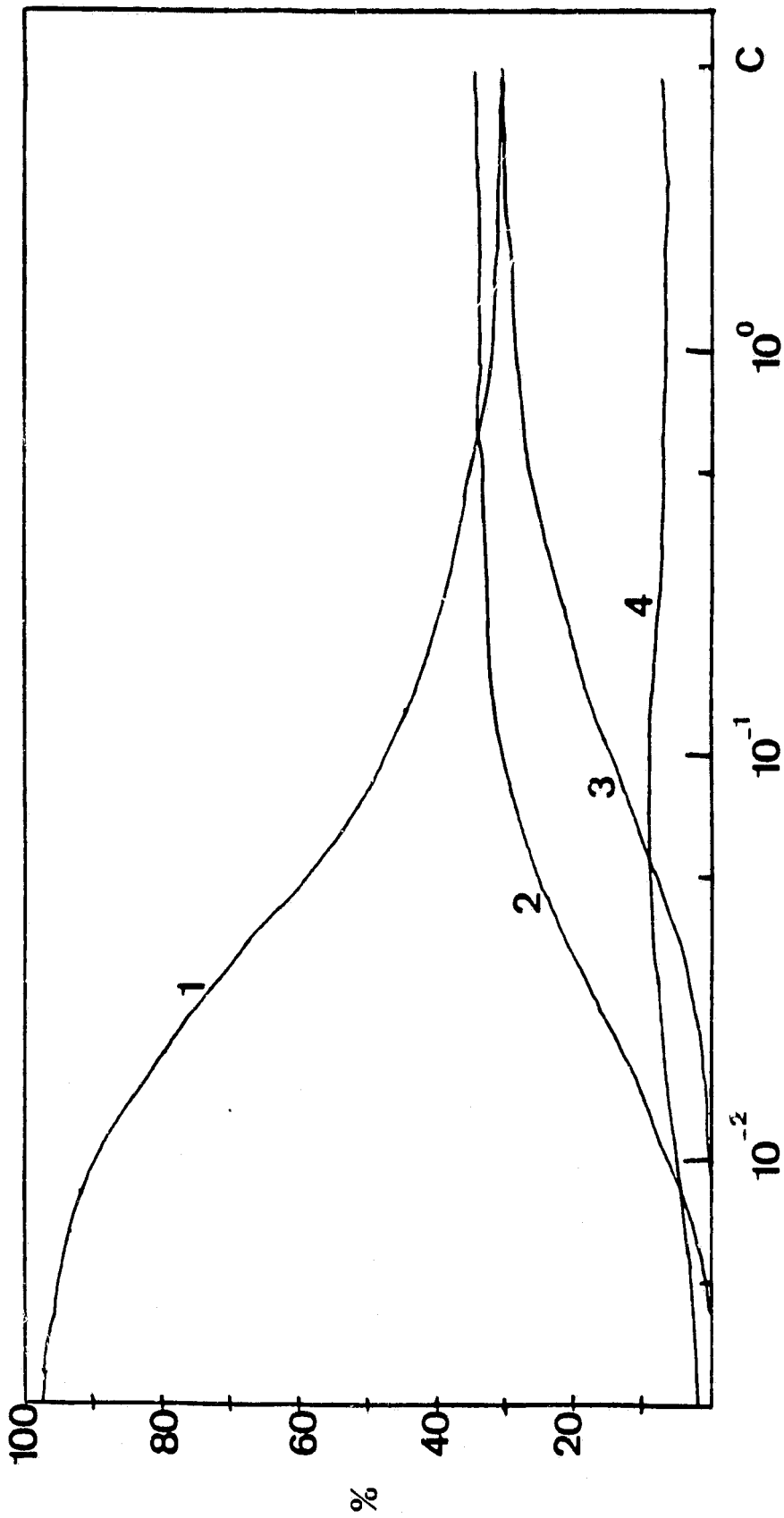

Figure 1 - Percentage distributions of free and complexed zinc as function of molar concentration of $ZnCl_2$. Curves 1, 2,3, 4 refer respectively to Zn^{2+}, $ZnCl^{+}$, $ZnCl_2$, $ZnCl_4^{2-}$.

In addition to the equilibrium equations (1-3), one can write those of conservation of zinc and charge neutrality. These equations were solved (for details, see Appendix I) and the results are shown in fig. 1. Mean activity coefficients were also available in the litterature and were taken into account to correct for departure from ideal solution behavior. As long as one sticks to binary electrolytes, it appears that there is no concentration for which a single dominant ionic species is present in the solution.

This situation is unacceptable because the presence of a mixture of complexes increases the number of unknowns in further experiments.

One immediately thinks of displacing the complexation equilibria (1-3) towards the fully complexed state by adding more chloride ions as an inert supporting electrolyte, e.g. NaCl. The only equation altered by this addition is that of charge neutrality in which the concentration of chloride ions $[Cl^-]$ is now a free parameter. It can be shown (see Appendix I) that the relative abundances of zinc complexes depend essentially on $[Cl^-]$. Given the dissociation constants, the ratio $[ZnCl_4^{2-}]/[ZnCl_2]$ is at least equal to 10 (the ratios with respect to lower order complexes are then even greater) as soon as $[Cl^-] > 0.5$ M. Since

$$[Cl^-] > \underbrace{[NaCl]_{total} - 2\times[ZnCl_2]_{total}}$$

remaining chloride ions if all zinc ions were converted to $ZnCl_4^{2-}$

one can take as a guiding rule : $[NaCl]_{total} - 2 \times [ZnCl_2]_{total} > .5$ M

In the present work, a constant concentration of inert electrolyte, [NaCl] = 3M, was finally selected, whereas the concentration of $ZnCl_2$ was

varied from 0.01 M up to 1 M. It is interesting to note that, in the concentrated solutions, where $[ZnCl_2]_{total}$ is not at all negligible with respect to [NaCl], zinc ions are still predominantly in the fully complexed state $ZnCl_4^{2-}$. This is because the abundance of complexes present in the solution depends mainly on the absolute value of $[Cl^-]$ and not on the Cl:Zn ratio.

I.3 - Titration Measurements

Zinc ions, due to their small size and double charge, are so polarizing, they can dissociate water molecules. They interact with hydroxyl groups and again can form complexes and polymeric networks. Complexes such as $ZnOH^+$, $Zn(OH)_2$, $Zn(OH)_4^{2-}$ are known to exist. In addition, in chloride solutions, chloride ions combine with these complexes and form low solubility oxychlorides[2]. In "pure" zinc chloride, these oxychlorides are soluble at high concentrations, precipitate upon dilution and redissolve upon further dilution[6].

No attempt was made here to elucidate this complex chemistry. However, it was necessary to determine the acid behavior of the solutions selected in the previous section. For this reason, titration measurements were carried out.

I.3.1 - Experiments

Excess droplets of concentrated HCl were first added to bring the pH to a very low starting value. Subsequently the solution was neutralized using a solution of sodium hydroxyde of comparable concentration. A magnetic stirrer kept the solution homogeneous. The pH-meter was an ORION ionalyzer 501 and the pH-electrode was a FISHER 13-639-90.

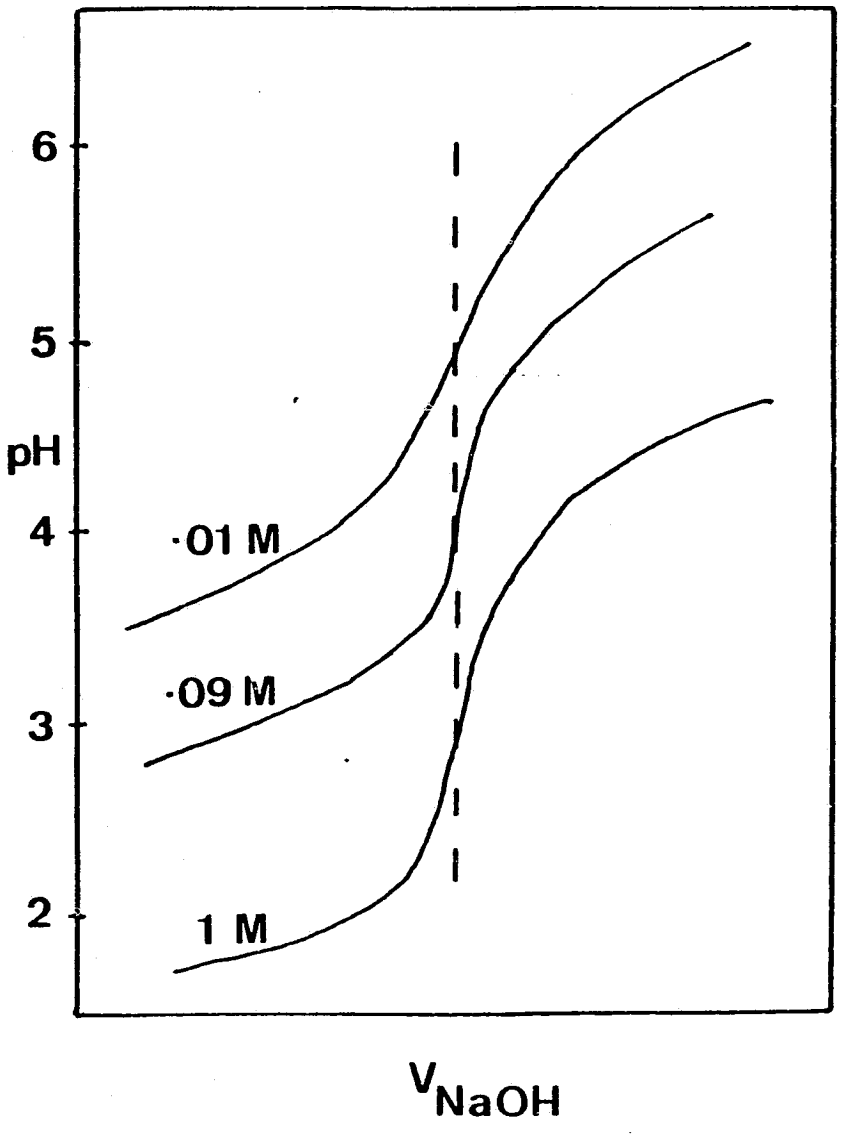

Figure 2a - Titration curves.

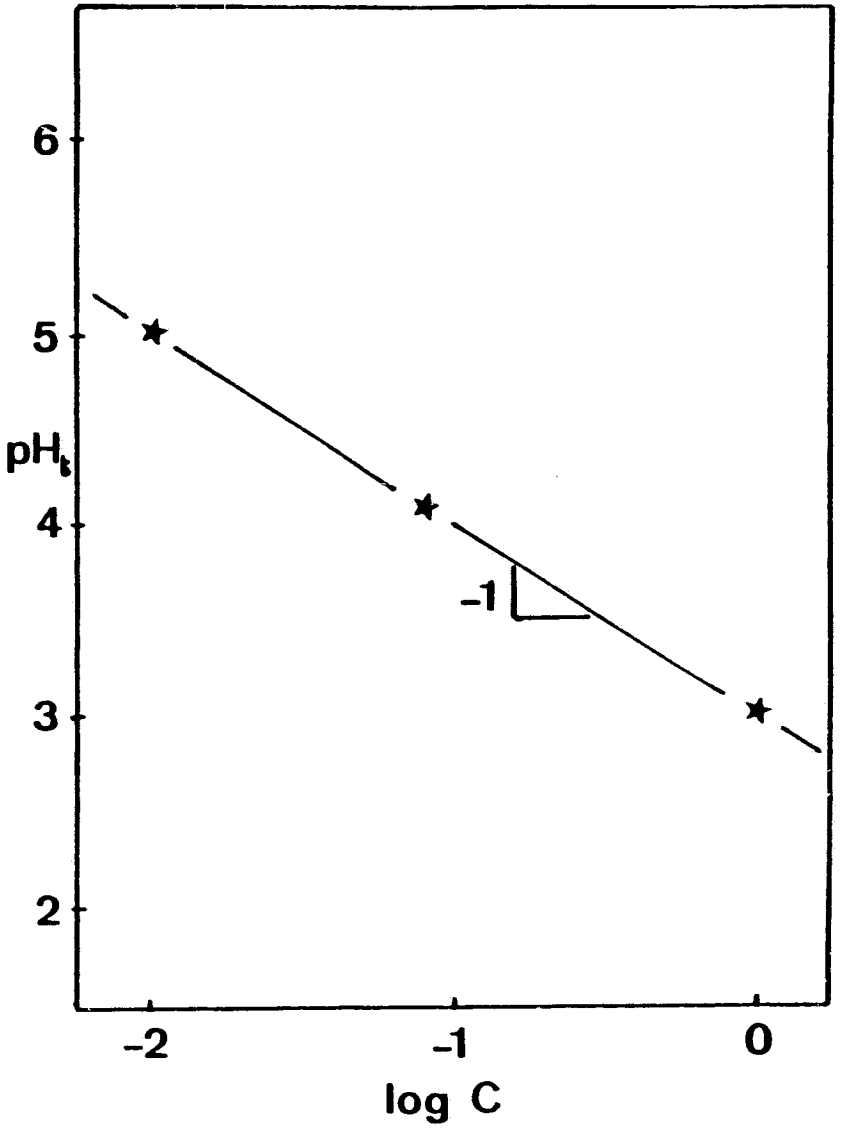

Figure 2b - A plot of pH_{tr} vs log C.

I.3.2 - Results and discussion

Fig. 2a shows the titration curves obtained. Upon neutralizing the excess of HCl, the pH rises sharply until the second acid present (i.e. zinc chloride) starts consuming the new hydroxyl groups. The inflexion point corresponds to $pH_{tr} = \frac{1}{2}(pK - \log C)$ where K is the dissociation constant of the weak acid and C its concentration. Indeed this transition occurs at higher and higher pH values as the concentration decreases. However the slope of pH_{tr} vs log C (Fig.2b) is -1 rather than $-\frac{1}{2}$, reminding us that $ZnCl_2$ does not behave as a simple weak acid either.

Of course one would like to work at pH values below the transition where there is too little of OH^- to form any oxychloride complex. The solutions used further had a pH that varied from 2.0 to 3.0 depending on the concentration of $ZnCl_2$. The pH was adjusted by adding droplets of concentrated HCl.

PART II : ZINC ELECTROCHEMISTRY IN ACID CHLORIDE BATHS

If interested in the kinetics of reactions taking place at the electrode surface, one can render the effect of mass transport negligible by working at low overpotentials and controlling the extent of the boundary layer. For instance, raising the rotation speed of a rotating electrode reduces the thickness of the hydrodynamic boundary layer so that deposition is only kinetics controlled.

On the other hand, if interested in mass transport, one rather works at overpotentials high enough so that the cathode behaves as an ion sink and maintains the surface concentration $C_s \approx 0$. Deposition is now limited by the transport of ions to the surface and the solution of the momentum/mass transfer equations gives the maximum possible current.

However in the case of zinc (as shown later on) dentrites start growing below the limiting current. Therefore we need understand both kinetics and mass transport properties of zinc deposition. Fortunately electrodeposition of zinc from aqueous solutions has been extensively studied both in acid and basic solutions [10-21] and a wealth of data is available in the litterature.

II.1 - Litterature survey

II.1.1 - Electroreduction of zinc

Although major studies were devoted to this topic over the last fifteen years, no general agreement was reached on the detailed mechanism of the reaction : $Zn^{2+} + 2e^- \rightarrow Zn$

LORENZ[10] suggested a simultaneous discharge of two electrons of adions

followed by their diffusion along the surface before they are incorporated in the lattice. But GAISER and HEUSSLER[11] showed that zinc deposition is first order. SIERRA ALCAZAR and HARRISON[12] put forward a reaction scheme consisting of two one-electron transfer steps, the first one being the rate determining step. This was confirmed by KIM and JORNE[13]. On the other hand WEBER and TOMASSI[14] proposed a mechanism involving zinc chloride complexes such as $ZnCl_3^-$, $ZnCl_4^{2-}$, $ZnCl_{2ads}$, etc ... EPELBOIN et al.[15-18] included an autocatalytic step :

$$Zn^{2+} + Zn^+_{ads} + e^- \rightleftharpoons 2\ Zn^+_{ads}$$

which accounted for multiple steady states that exist in a certain range of pH and overpotentials. Coupled with surface diffusion of Zn^+ adion, this autocatalytic reaction accounted also for the observed change in deposit morphology with overpotential.

The same ambiguity appears when dealing with basic solutions[19-21]. Here zinc is known to be present in the form of zincate ions $Zn(OH)_4^{2-}$ but again the details of the overall reaction : $Zn(OH)_4^{2-} + 2e^- \rightarrow Zn + 4OH^-$ remains unknown.

Despite this lack of agreement, many characteristics of the electroreduction of zinc are commonly admitted :

1) the importance of pH : the pH affects the polarization curves. Correlations such as $\eta = A + B\ (pH-7)$ at constant current were obtained[22]. A seems to be constant regardless of the anion whereas B depends strongly on the nature of the anion present. One order of magnitude difference in exchange current densities was reported for zinc in chloride solutions differing only by their pH value[23].

2) adsorbed hydrogen plays an important catalytic role in zinc deposition and may have an indirect effect by partially covering the electrode surface[14].

3) codeposition of hydrogen exists at all overpotentials. This is supported by the dependence of coulometric efficiency on pH[15], by the detection of traces of hydrogen bubbles even at low overpotentials [24], and by the absence of plateaus in current-overvoltage curves due to early hydrogen evolution[13].

To the author's knowledge, nobody in the litterature tried to take into account the chemistry of zinc chloride in their attempt to understand the mechanisms of zinc deposition in chloride solutions (though some investigators were aware of its complexity). This may be surprising after what was showed in Part I and could be only attributed to a lack of communication between chemists and electrochemists. Actually several discrepancies could be simply explained in terms of bath composition. Changes in pH value of course alter the ratio of adsorbed hydrogen relative to other adsorbed species but can also affect the relative abundance of the ions present in the bulk and containing zinc atoms. Those ions have different overall charges and most probably different geometries. Therefore it is no surprise they have different electrochemical behaviors. This explains the unusual difference in exchange current densities reported by some authors as well as the dependence of polarization curves on pH.

For similar reasons, one cannot truly compare results obtained from solutions having different Zn/Cl ratios because the chloride complexes would be also present in different ratios. Even when the Zn/Cl ratio is kept constant, say 1:2 for binary electrolytes, the bath composition

is not the same whether the concentration of the solution is 10^{-2}, 10^{-1} or 1 M(see Part I).

II.1.2 - Deposit morphology

Zinc system is one of the most used in the study of electrodeposit morphology. Indeed, from the industrial standpoint, controlling the quality of zinc deposits is critical in such applications as protective corrosion-resistant coatings and batteries. From the academic standpoint, various morphologies are readily obtained as the current density is increased : mossy, compact, dentritic and powdery. A comprehensive analysis of deposition shows that among the three components of overpotential (activation η_a , ohmic η_Ω , concentration η_c), only activation overvoltage contributes to keep the surface smooth. η_Ω and η_c arise due to difficulties in ionic transport whether by migration (η_Ω) or diffusion-convection (η_c) and are responsible for surface instabilities. Deposition is never migration controlled in aqueous solutions but could be at low currents in molten salts. A case where deposition is diffusion controlled is of course at the limiting current.

Some authors( ) phenomenologically correlated surface roughness with i/i_1 ratio where i_1 is the limiting current. Others put forward more basic theories to explain dentrite growth. BARTON and BOCKRIS[25] derived a theory based on optimum radius of curvature of a dentrite tip as a function of overpotential (optimum in the sense of growth rate). Two consequences of their work were the identification of a critical overpotential below which dentrites cannot grow and the presence of an induction time before dentrite growth takes place. The dependence of these quantities on concen-

tration, overpotential, etc... was predicted and checked experimentally. DESPIC and POPOV[26] in a review article suggested a model based on surface roughening, making little difference between small asperities and dentrites. Their model resulted from investigations made precisely on zinc electrodeposition. IBL[27] also proposed similar explanations and reviewed results concerning powdered electrodeposits. AOGAKI et al.[28] rationalized the observations using linear instabilities theories similar to those of MULLINS and SEKERKA[29].

BOCKRIS and DESPIC[30] were surprised of such a big difference in critical overpotentials (η_{Cr}) between silver and zinc -respectively 3 and 80 mV-. Further investigationes confirmed the fact that η_{Cr} is specific of each metal and could vary from a few millivolts to several volts[31]. The conventional thermodynamic representation of η_{Cr} as an energetic barrier was unsatisfactory. Indeed nothing in the crystallographic properties of these metals could account for such variations. DESPIC[32] pointed out that metals with increasing η_c are in the same sequence regarding current densities and suggested instead a kinematic representation: η_{Cr} would be the potential for which the induction time suddenly increases beyond reasonable experimental times.

If the kinematic representation was correct, the same metal deposited from different ionic species should have different critical overpotentials (because the exchange current densities are different). This was indeed the case for zinc : deposited from zincate ions ($Zn(OH)_4^{2-}$), it had an η_{Cr} = 80 mV[30], whereas, deposited from sulfate solutions (hydrated Zn^{2+}), it had an η_{Cr} =170mV[33]. In the present work, zinc was deposited from fully complexed $ZnCl_4^{2-}$ ions. Therefore the corresponding critical

overpotential, presumably different from both values mentionned above, had to be determined experimentally.

II.2 - Experiments

The experimental set-up is shown schematically in fig. 3. The cell was made out of plexiglass. The anode was cut out of a sheet of pure zinc (Alfa 99,99 %) 10 mils thick. The cathode was a preplated platinum wire 10 mils in diameter similar to that used by POPOV[33]. The preplating was carried out at low current densities and over a time long enough as to obtain a continuous smooth layer of zinc. If the layer was not continuous it would have been rapidly corroded : Pt has a very low hydrogen overpotential whereas Zn has a fairly high hydrogen overpotential. The result is a complete corrosion cell where preplated zinc is dissolving and hydrogen is evolving on bare platinum wire. A stable potential of the plated wire (which behaves now as a zinc wire) with respect to a reference electrode meant that the layer was indeed continuous.

Two kinds of solution were used. They had the following compositions :

3 M NaCl, 1 M $ZnCl_2$, pH = 2

3 M NaCl, 0.1 M $ZnCl_2$, pH = 2.5

Deposition experiments were done potentiostatically and the current was recorded vs time. The reference electrode was a standard calomel electrode FISHER 13-639-52. The potentiostat was an AARDVARK V-2LR. The chart recorder was a HEWLETT-PACKARD 7100BM.

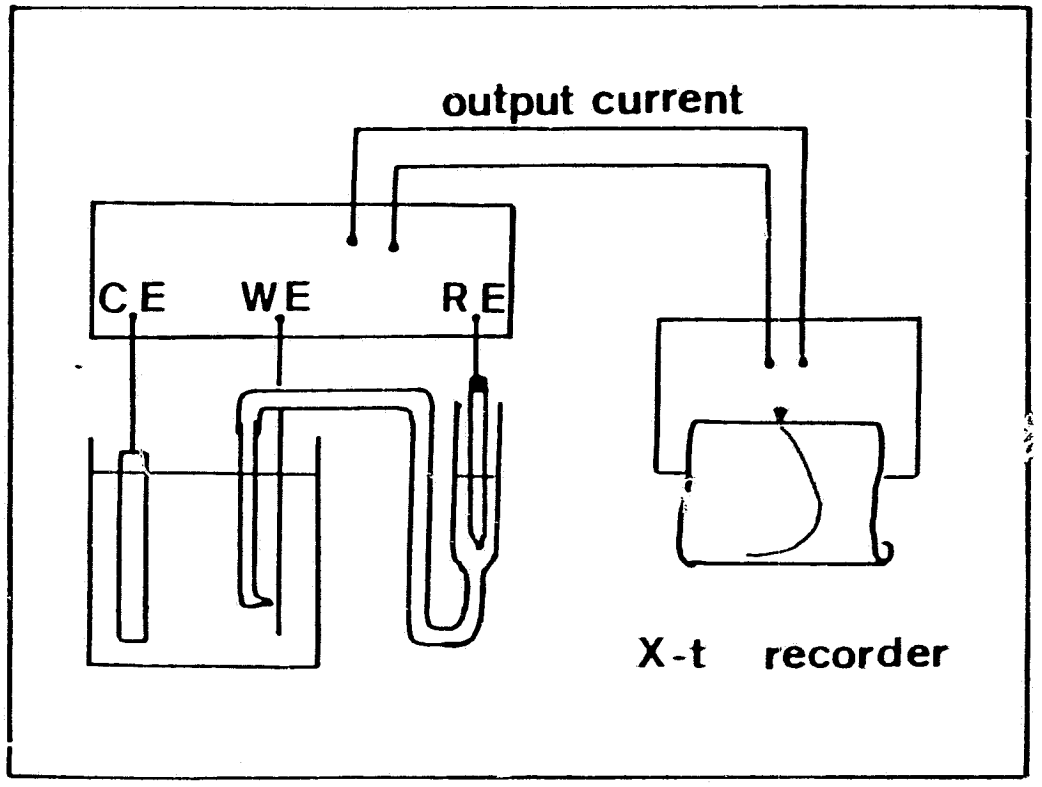

Figure 3 - Experimental set-up for the determination of the critical overpotential.

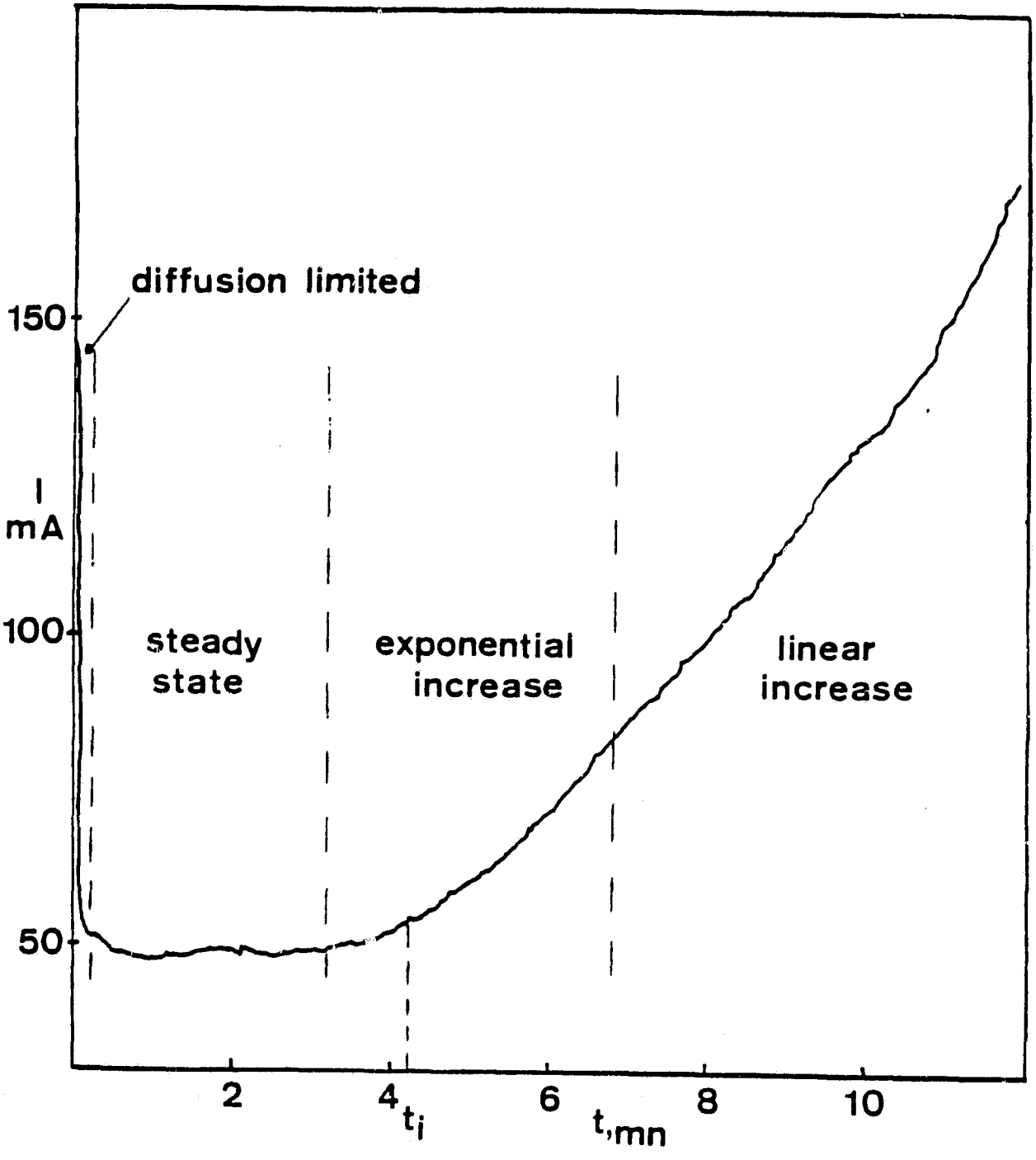

Figure 4 - A recording of current vs time for the determination of the critical overpotential. Solution contains 1 M $ZnCl_2$; overvoltage = 150 mV.

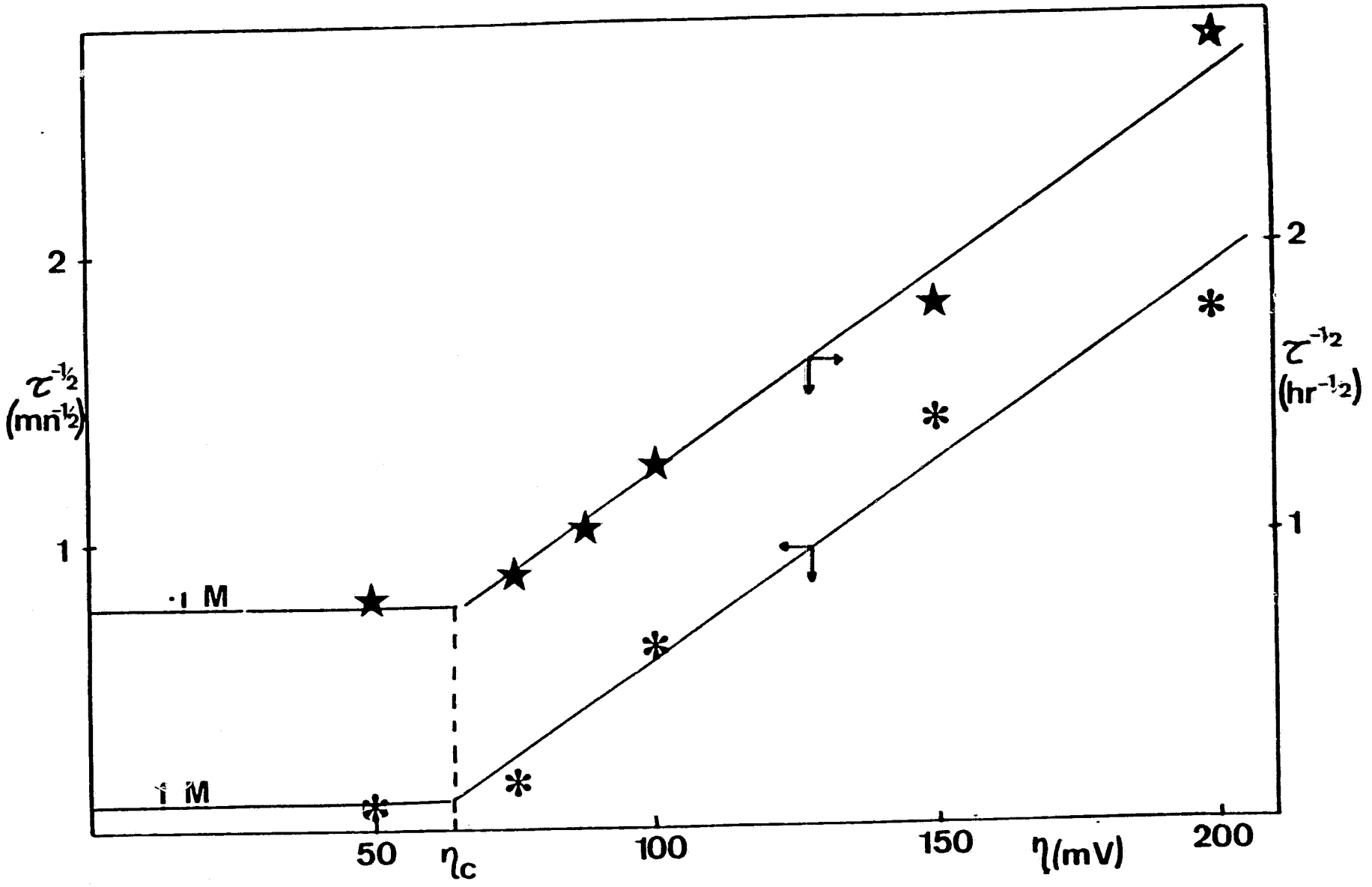

Figure 5 – A plot of time constants of surface roughening vs overpotential.

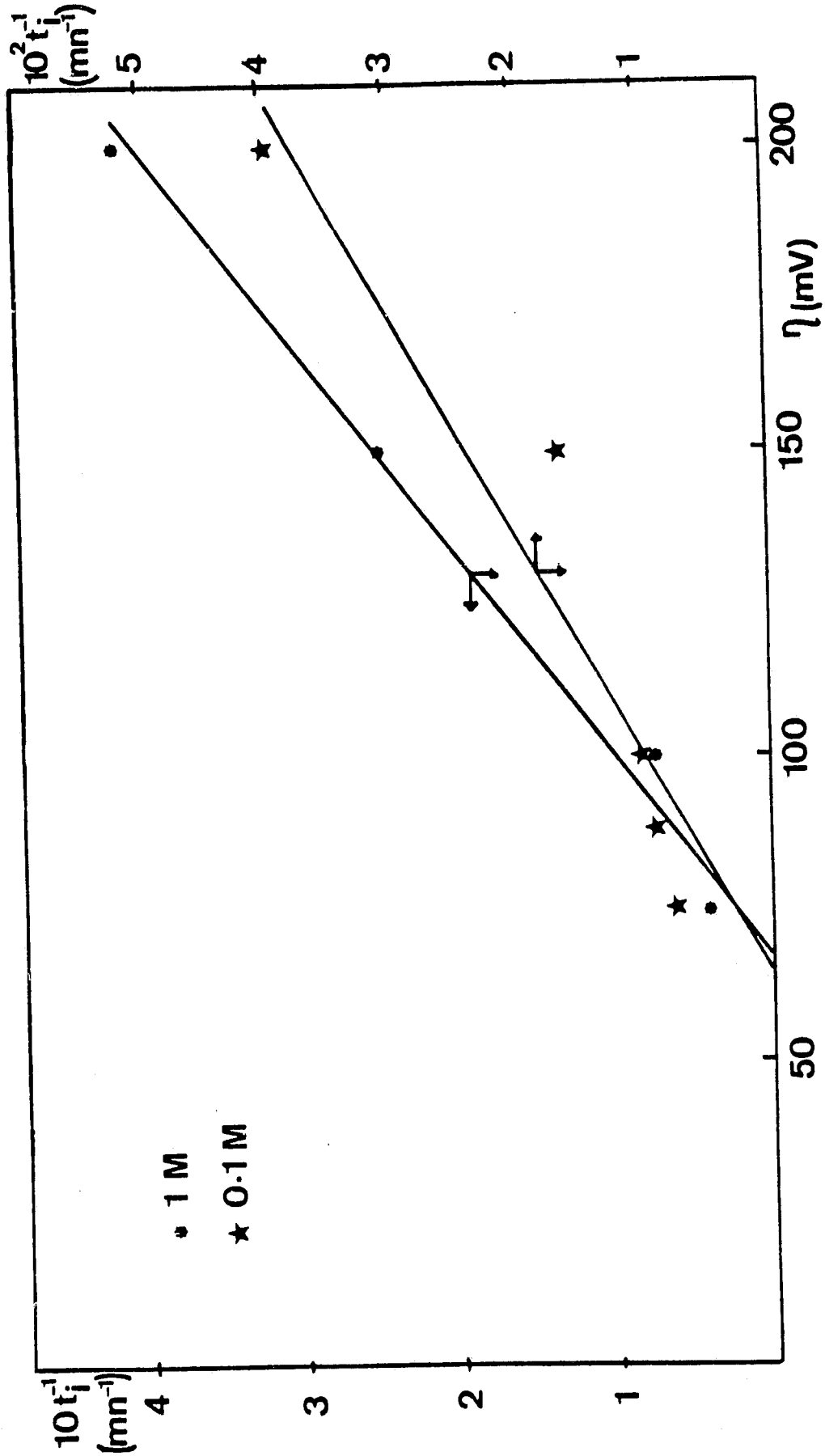

Figure 6 - A plot of induction times for dentrite growth vs overpotential.

II.3 - Results

Fig. 4 shows a typical curve of current vs time. The current first decreases due to diffusion, reaches a steady state ans stays constant for a while then starts increasing due to dentrite growth. The increase is first exponential then linear.

From such a curve, two quantities were extracted :

1. an induction time : defined as the time at which the current increased 10 % with respect to its minimum value.

2. a time constant, associated with the exponential increase of current. The section of the curve of varying positive slope was fitted to an exponential (the exact procedure is discussed in Appendix II) and a time constant was deduced . The fit was usually very good (correlation coefficient > .97).

Results are plotted in fig. 5 and 6. Both induction times and time constants suggest a transition around η_c = 65 mV. A one order of magnitude increase in concentration lowered considerably the induction times and time constants (by a factor of 8 roughly) but did not change the value of the critical overpotential.

PART III : CONVECTIVE FLOW DURING ZINC ELECTRODEPOSITION

The performance of an electrolysis cell (efficiency, deposit quality, higher attainable current densities) is usually limited by the supply of ions to the electrode surface.

If diffusion was the only way to supply ions, deposition could not be maintained very long : in a galvanostatic mode, the ions close to the electrode are reduced first, ions located further away need time to reach the surface. The result is a local shortage of ions. The potential rises sharply in order to keep up with the required current until a second cathodic reaction takes over (typically hydrogen evolution). In a potentiostatic mode, as the boundary layer is depleted the current drops and soon becomes virtually equal to zero.

Fortunately, due to concentration gradients, a convective flow near the electrode is usually present. It brings fresh solution to the electrode and maintains a non-zero steady state current.

In addition, other means were devised in order to enhance mass transport :

1) forced convection with a variety of stirring modes : inert gaz bubbling, hydrogen evolution, magnetic stirrers, ultrasonic waves, ...

2) modulation of the applied voltage/current : pulses, square waves, ac perturbations superimposed on a constant value have been already tried and many others.

3) rapid motion of the cathode : rotating electrode, running-wire, etc, ...

4) flowing electrolytes, impingements of the electrolyte on the cathode, etc ...

Few of these solutions found industrial applications because they were either impractical or costly. It is the purpose of this work to show that a rational cell design by enhancing free convection can substantially improvemass transport during electrolysis.

III.1 - Litterature survey

A theoretical treatment of convective mass transfer is fairly recent. It is an important problem in chemical engineering and naturally chemical engineers were the first interested in it .. Now a standard technique to study mass transfer is precisely an electrochemical one called the limiting current technique. It was recently reviewed by SELMAN and TOBIAS[34]. AGAR[35] applied dimensional analysis to the diffusion convection processes near the electrode surface and extended results by analogy from theoretical and experimental work on heat transfer. Free convection at vertical electrodes was then studied by WAGNER[36-37]; TOBIAS[38-39] and IBL[40-41]. More recently convection at horizontal and inclined electrodes was investigated by WRAGG[42-46]. In all cases, correlations between the usual dimensionless quantities (Sherwood, Grashof and Schmidt numbers) were obtained for laminar and turbulent regimes. They fit reasonably well theoretical predictions. The results reported in the litterature can be summarized as follows :

- Depending on the orientation of the electrodes and Rayleigh number (= Gr × Sc), different flow regimes can take place with the onset of instabilities in the transition ranges.

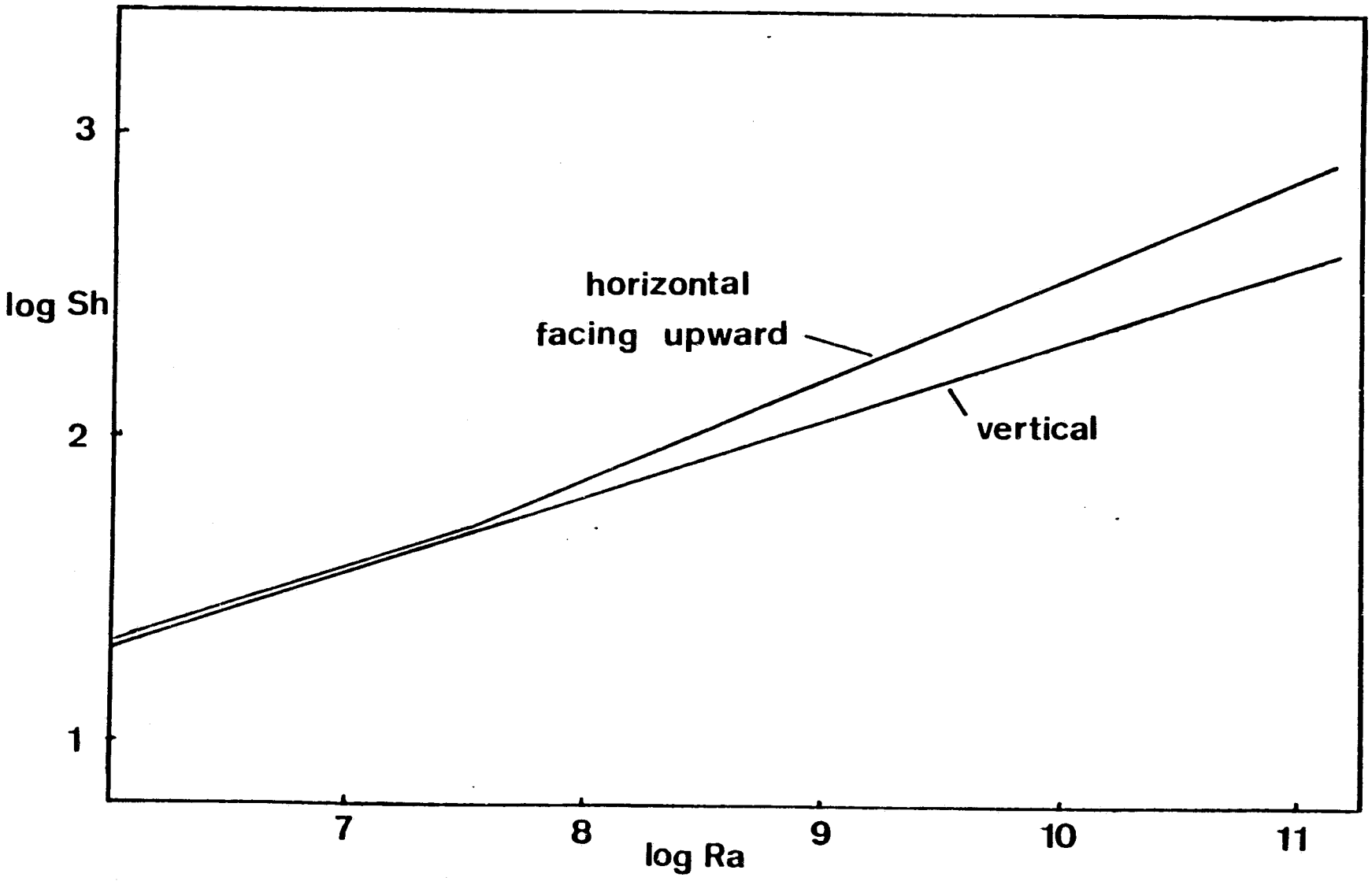

Figure 7 - Effect of electrode orientation on mass transfer.

- SPARROW[47] taking the boundary layer thickness as a characteristic length gives a threshold value of Ra (1800) below which free convection is not possible.

- laminar attached boundary layer flow is well correlated with $Sh = 0.66\ Ra^{1/4}$. This is the case of vertical electrodes and downward facing electrodes. The relation stays valid for fairly large Ra numbers.

- for $Ra > 2.5 \times 10^7$, turbulent detached boundary layer flow develops above upward facing electrode and is well correlated with : $Sh = .16\ Ra^{1/3}$ (indicating that mass transport becomes independent of electrode dimensions).

In the series of work mentionned above, the authors were mainly interested in the mass transfer problem regardless of cell performance or deposit quality. To the author's knowledge, the only attempt to understand the effect of convection on cell efficiency was that of SELMAN et al.[48] in their study of mass transfer around a rod-shaped electrode.

Clearly convection is extremely geometry sensitive. Depending on the orientation and shape of the electrode, convection could be favored or unfavored. Fig. 7, taken from Ref. 45 , shows how mass transport is enhanced just by changing the orientation of the electrode from vertical to horizontal facing upward. The enhancement is more and more pronounced at high Rayleigh numbers. This is precisely the range of practical interest since it corresponds to electrode dimensions larger than a centimeter.

III.2 - Description of experiments

The interaction of convective flow, concentration and current was studied below and at the limiting current for different electrode configurations. It was shown in Ref. 45 , that horizontal upward facing cathodes have the best orientation, as far as mass transfer is concerned. Consequently, in the present work, only horizontal electrodes were considered.

Convection at upward facing cathodes arises because during deposition, the boundary layer, poor in solute, is lighter than the bulk. Beyond a certain thickness of the boundary layer, this situation is hydrodynamically unstable : electrolyte from the bulk falls toward the cathode whereas light electrolyte from the boundary layer rises. Conversely, at downward facing anodes, the rich solution in the boundary layer is too heavy, it sinks to the bottom and is replaced by fresh solution from the bulk.

Fig. 8 shows the three electrode configurations that were studied. In the TF (top free) arrangement, the anode is placed below the cathode and is facing downward so that its dissolution does not perturb the flow pattern near the cathode. The AT (anode on the top) configuration combines the two convective flows, the one due to cathodic deposition and the one due to anodic dissolution. Finally the G (for grid) set-up is expected to represent an improvement on the previous arrangement : the cathode, which is now a grid, is not anymore an obstacle to the falling electrolyte. The mixing of the upward and downward convective flows is therefore more vigorous near the cathode surface and insures a more efficient stirring. In addition, the boundary layer, with its new cylindrical geometry and a thickness on the order of the radius of curvature of the cathode surface, can

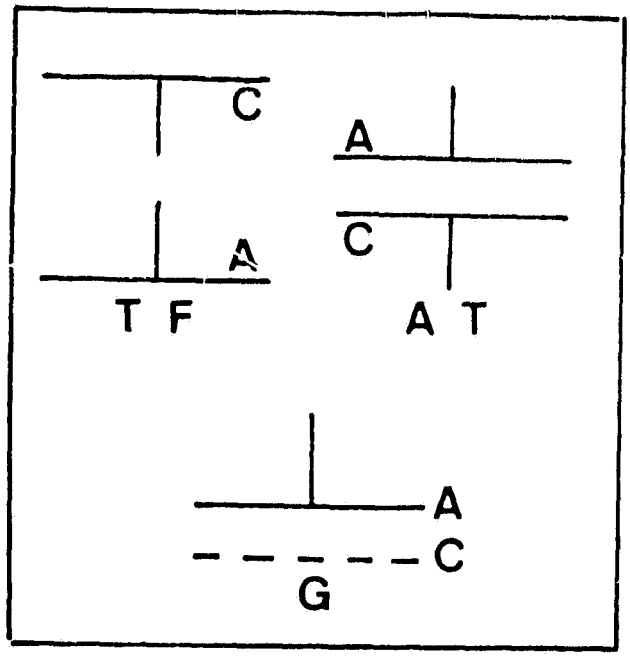

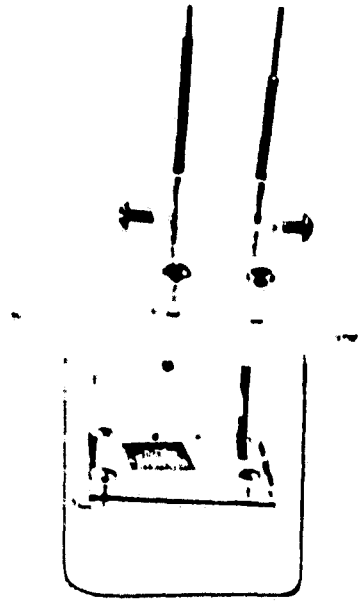

A T

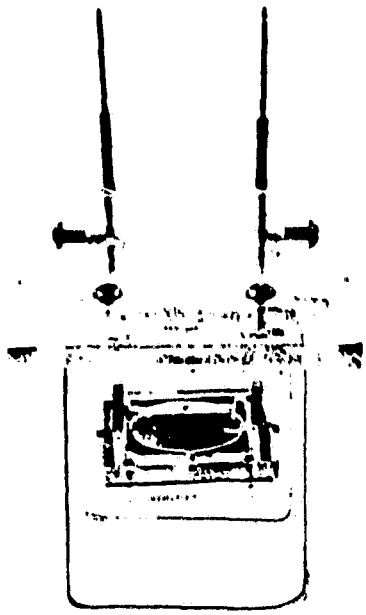

T F

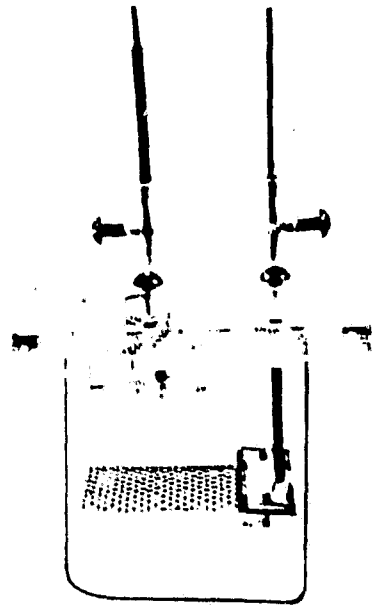

G

Figure 8 - Electrode configurations used in the study of convection

be more readily perturbed and fresh solution can reach more easily the electrode.

Deposition was carried out potentiostatically in all three cases, and current was recorded continuously vs time. Both transients and long time deposition were studied for a wide range of overpotentials and concentrations.

Flow patterns were observed visually using a standard laser schlieren technique. During transients, photographs were taken regardless of the current that was recorded simultaneously. However, an event marker recorded on the chart paper the precise time at which each photograph was taken. Thus it was possible to establish correlations between the evolving convective flow and features on the current-time curve.

III.3 - Technical details

III.3.1 - Electrochemical equipment

The electrochemical cell was a glass 2" - sided cubic cell. It had two transparent faces of optical quality. A plexiglass cover was designed and machined so that it fits on the top of the cell. It served also as a platform along which the electrode holders can slide so that the distance between them can be adjusted. Different electrode holders had to be designed and machined for each electrode configuration. Fig. 9 shows a side view and a top view of the TF electrode holder. Similar ones were used for other configurations. They are shown with the cover in fig. 10.

Both anode and cathode were pure zinc (99,99 %) discs 1" in diameter and 10 mils thick. They were polished first mechanically using emery paper grade 600 to remove a protective layer of zinc hydrocarbonates from the surface. They were then dipped in 50 % HCl solution for a few seconds. Finally they were rinsed, installed as wet on the electrode holder and immersed in the solution as soon as possible. In the case of the G configuration, the cathode was chromel grid (40 mesh units/cm^2) preplated in the same conditions as the Pt wire in Part II.

Based on investigations discussed earlier in Part I, five solutions were used. They were labelled from I to V with decreasing concentration of zinc chloride. They had the following compositions :

I	II	III	IV	V
3M NaCl	3M NaCl	3M NaCl	3M NaCl	3M NaCl
1M $ZnCl_2$	0.3M $ZnCl_2$	0.1M $ZnCl_2$	0.03M $ZnCl_2$	0.01M $ZnCl_2$
pH=2.0	pH=2.2	pH=2.5	pH=2.7	pH=3.0

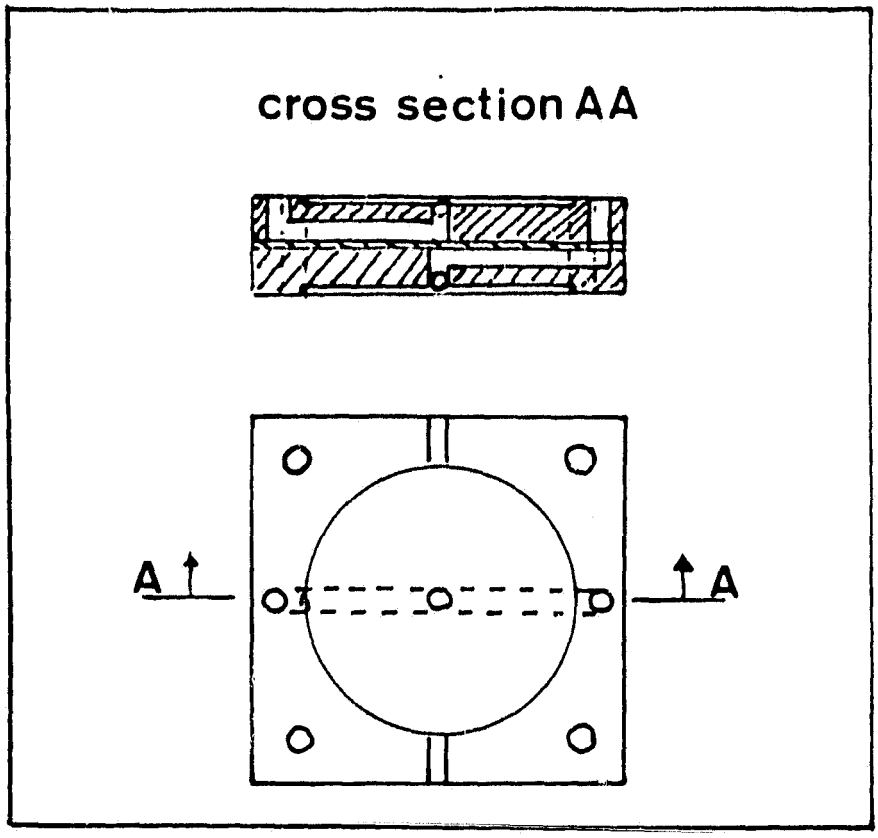

Figure 9 - Top view and side view of the TF electrode holder.

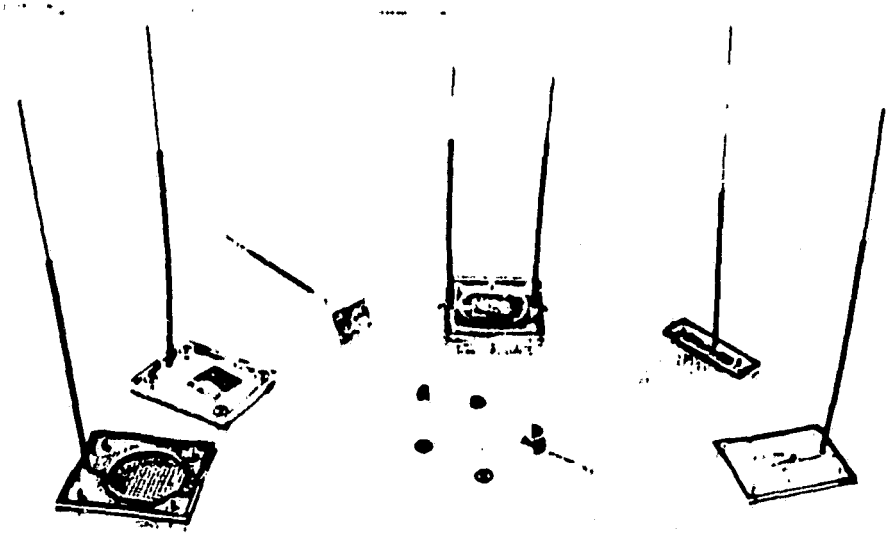

Figure 10 - Cover and electrode holders used.

The pH was adjusted by adding droplets of concentrated HCl. Only FISHER analytical grade salts were used. The reference electrode was a standard calomel electrode. It was connected to the electrochemical cell through a salt bridge at the end of which a Luggin capillary approached the cathode surface as much as possible (< 1mm).

The potentiostat used was an AARDVARK model V-2LR. And whenever the current was close to 1A (with solution I) a power booster (AARDVARK model X) was added. The X-t recorder was a HEWLETT-PACKARD model 7100 BM. All instruments were recalibrated at the beginning of the experiments.

III.3.2 - Optical equipment

Schlieren methods[49] are standard visualization techniques used in the study of fluid flow. They rely on changes in density of the investigated medium (due to temperature or/and concentration gradients, or pressure gradients in compressible fluids). Their use by electrochemists has been very limited[50-52] but several recent works suggest a "rediscovery" of this valuable tool[53-55].

The idea is simple. A light source shines on the investigated medium and a real image of it is made further away. At the focal plane, a knife edge is introduced. If the medium is perfectly homogeneous, the image disappear upon inserting the knife edge. If the medium is not homogeneous, each elementary volume diffracts light in a slightly different direction (because of a different index of refraction). Some light rays will be able to bend around the knife edge and an image is still recorded. The inhomogeneities show up as bright on a dark background. The contrast of the image depends on how much light rays are deflected which is in turn proportional

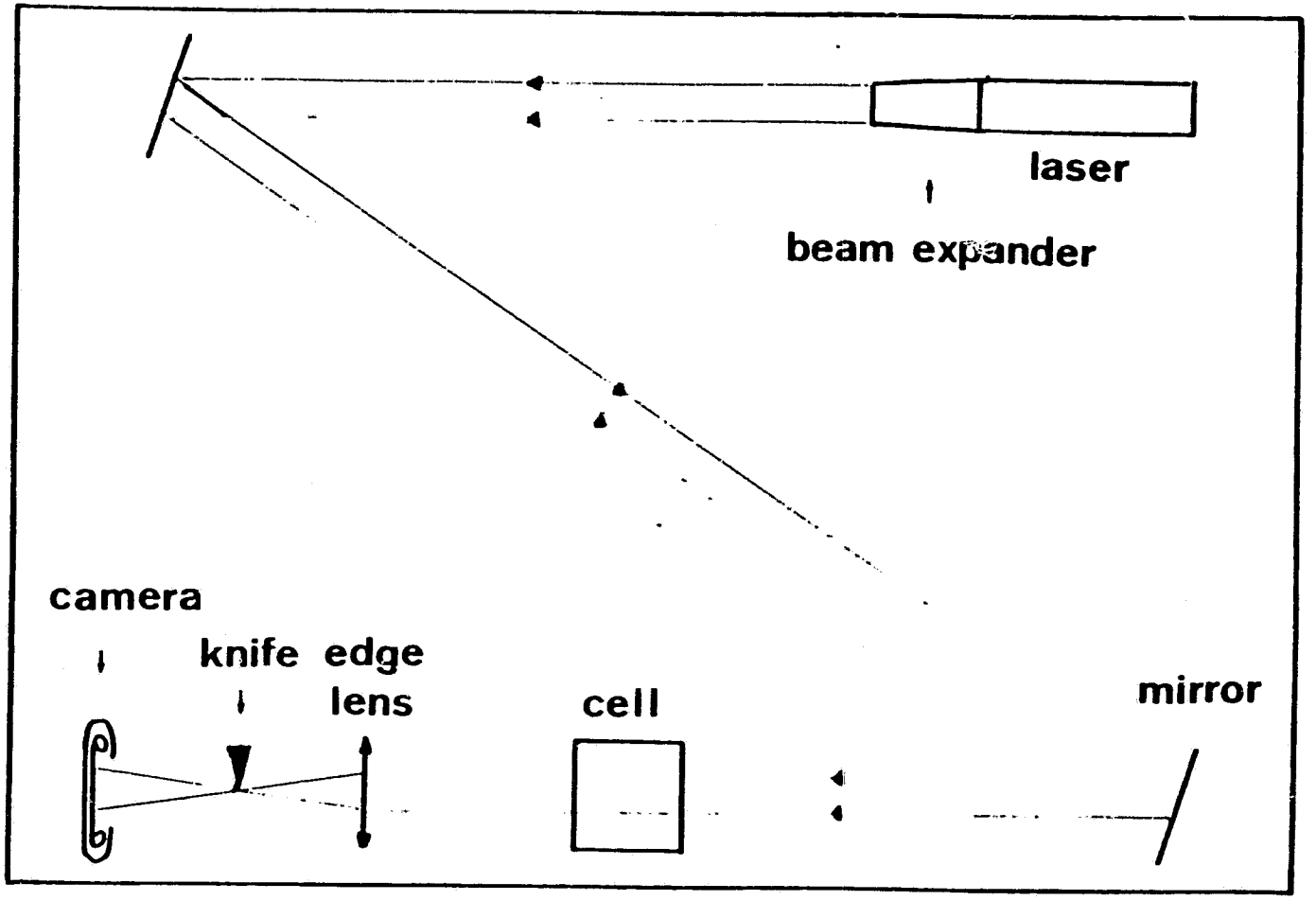

Figure 11 - The schlieren set-up in a z-configuration.

to the concentration gradients in the bath.

All the optical equipment and the cell were mounted on a vibration free 6'×4' optical bench (NRC RS -46-8). A Z- configuration, which would be convenient for both aqueous and molten salt experiments was finally selected. The optical arrangement is shown schematically in fig. 11. The light source was a MELLES-GRIOT 10 mW helium - neon laser. The initial .8 mm beam was expanded up to 28 mm, NRC mirrors reflected the beam twice and a lens (ORIEL 4263) of 120 mm focal length focused it. The cell itself was gripped in a vice for stability reasons and was installed on a lab jack. The latter allowed an easy adjustment of its level with respect to the laser beam. At the focal plane, a razor blade was positionned. It was mounted on an x-y-z translator for fine position adjustment. The film plane of a lens-less NIKON FE camera was placed at the image plane of the electrodes. A motor drive NIKON MD12 controlled by a cable release enabled trouble-free fast rate photography. The films were 36 exposure KODAK TRX-135.

III.4 - Results and Discussion

III.4.1 - Transients

Fig. 12 shows a typical I vs t curve. Initially the current decreases rapidly from a theoretically infinite value due to diffusion. Eventually the boundary layer becomes thick enough for convection to take place. As soon as convection starts, the supply of fresh solution from the bulk increases the current. After a while a steady state is reached and the current is stable. From such a curve, several useful quantities can be obtained :

1) the steady state current i_{ss} is a measure of how efficient

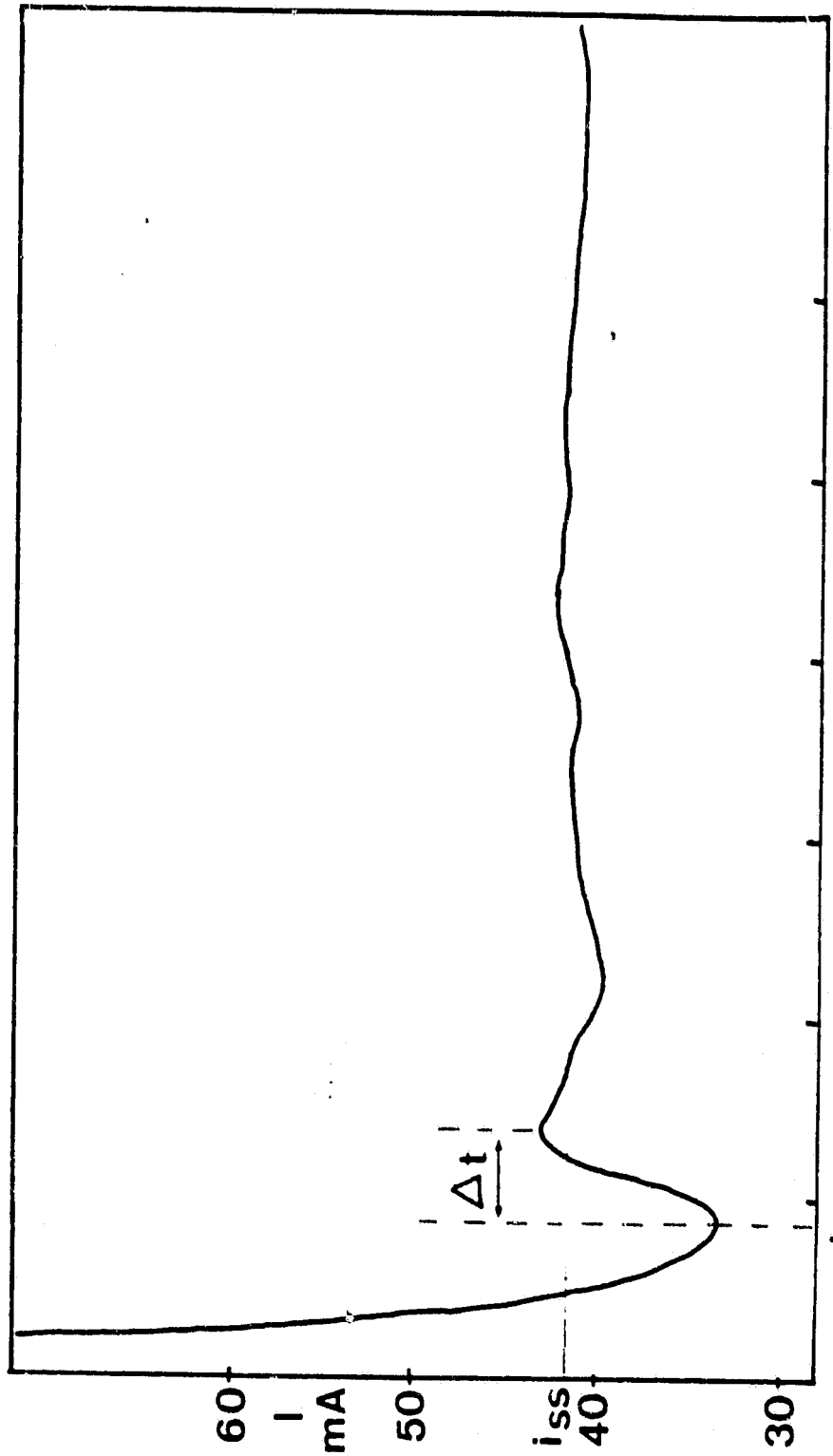

Figure 12 - A typical I-t curve in the study of transients. (Solution III ; overvoltage = 75 mV ; TF configuration).

convection is in bringing additional ions to the surface.

2) the time t_{min} corresponding to the undershoot. This time indicates the moment at which pure diffusion to the cathode surface becomes hydrodynamically unstable.

3) the time span Δt between the minimum and the maximum gives a good idea of how fast an elementary volume is brought to the surface, is depleted and carried away back to the bulk.

III.4.1.1 · The TF configuration

Of the five solutions used only four exhibited a behavior as the one illustrated in fig. 12. In the case of solution V which contained the least of $ZnCl_2$ (0.01 M), the current kept decreasing monotonically, suggesting that convection could not occur (laser schlieren did not reveal any convective flow either). Diffusion was presumably the only mechanism by which ions reached the surface. Such curves were used to obtain a diffusion coefficient for $ZnCl_4^{2-}$ in this kind of solution. The curves were replotted as I vs $t^{-1/2}$ and extrapolated to the origin ($t \to \infty$). The slope gave $D = .7 \times 10^{-5}$ cm^2/s after the formula :

$$I_{dif} = nFA \sqrt{\frac{D}{\pi t}}$$

where F is Faraday's constant, A the electrode area.

Fig. 13a shows the i_{ss} - V curve in the case of solution III. The curve has two interesting features. First the rapid linear increases at low overvoltages, secondly, to the contrary of what has been reported so far, a well-defined plateau exists at high overpotentials. Thus with this

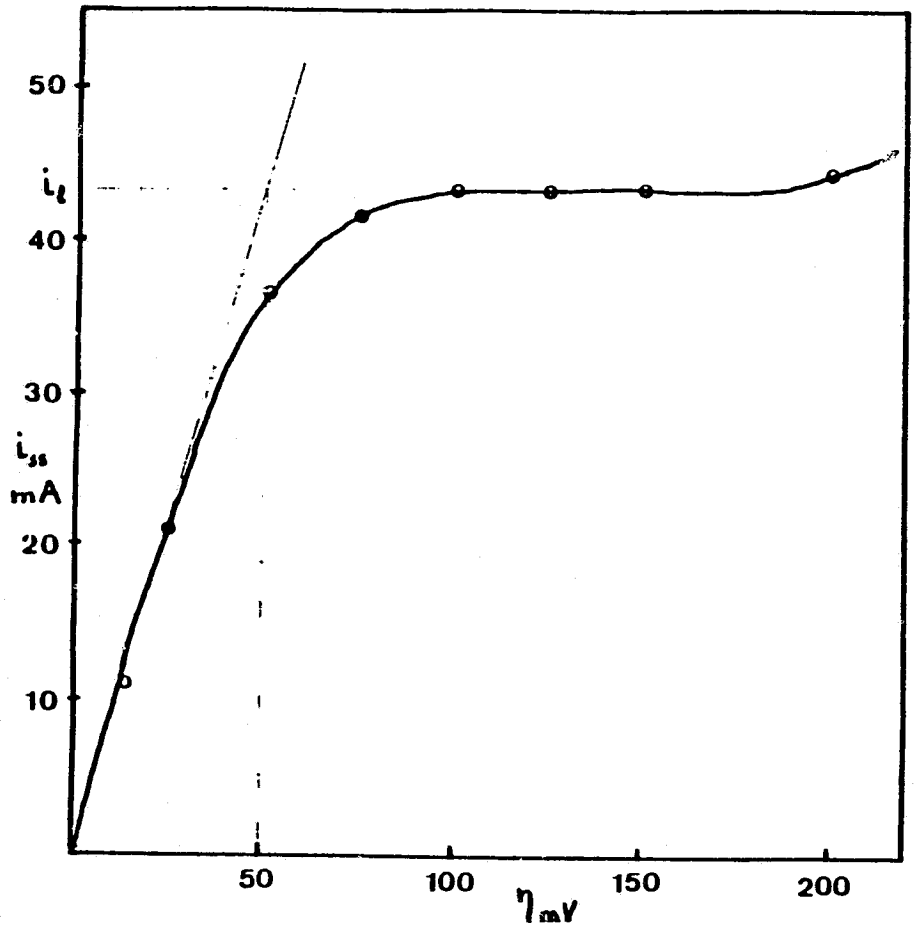

Figure 13a - The i_{ss}-V curve in the case of solution III with the TF configuration.

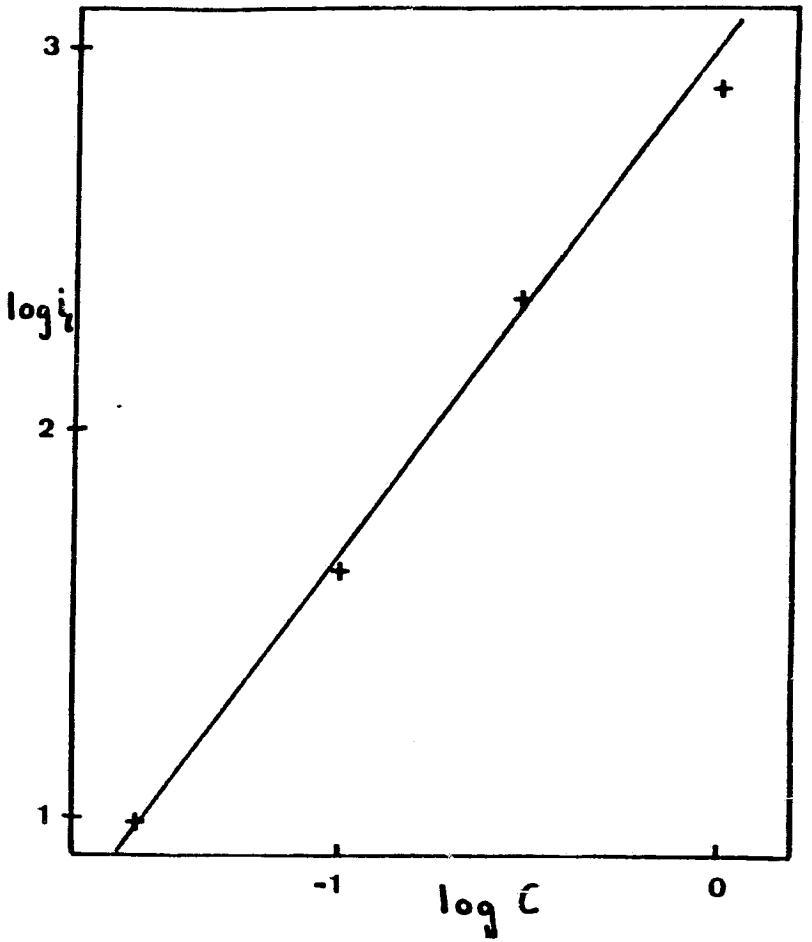

Figure 13b - A log-log plot of the limiting current vs concentration.

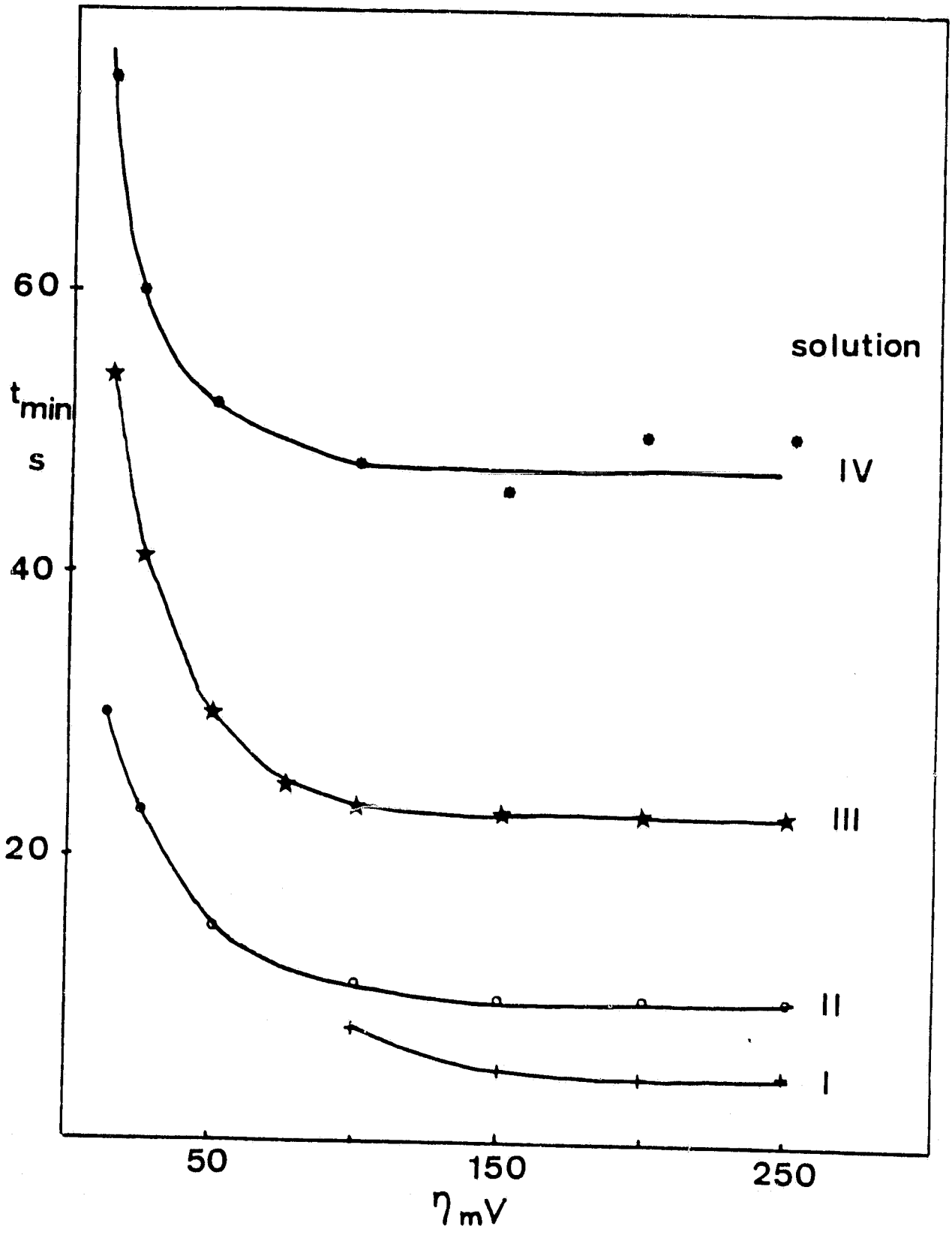

Figure 14 - Convection initiation time vs overpotential in the TF configuration.

geometry and with this kind of bath, hydrogen evolution has been successfully inhibited. Similar curves were obtained for the other solutions : of course the absolute value of current changed with concentration but in all cases, there was first a rapid linear increase then a well-defined plateau. Extrapolation of both segments gives a transition overpotential around 50 mV. Fig. 13b shows a log - log plot of the limiting current vs concentration. The correlation is fairly good and follows :

$$i_{l(A)} = 1.0\ C_{(M)}^{4/3} \qquad \text{(III.3)}$$

This relation, converted into dimensionless quantities becomes :

$$Sh = 0.14\ Ra^{1/3} \qquad \text{(III.4)}$$

In this conversion the following numerical values were used :

- the electrode area $A = 5.07\ cm^2$
- the densification coefficient $\gamma = 0.11\ M^{-1}$ (from data on pure zinc chloride [4])
- the kinematic viscosity $\nu = 1.3\ cS$ (estimated viscosity from data on NaCl solutions [7])

Relation (III.4) is in excellent agreement with relation obtained by WRAGG[43]. It means that mass transfer is independent of electrode dimensions and indicates that convection is turbulent (if it was laminar, $Sh \propto Ra^{1/4}$ and i_l would have been proportional to $C^{5/4}$).

Fig. 14 shows t_{min} as a function of overpotential. At low overpotentials t_{min} is large and decreases rapidly to reach a steady state value $t_{min,l}$ at the limiting current. $t_{min,l}$ is plotted vs concentration in fig. 15 and is well correlated with :

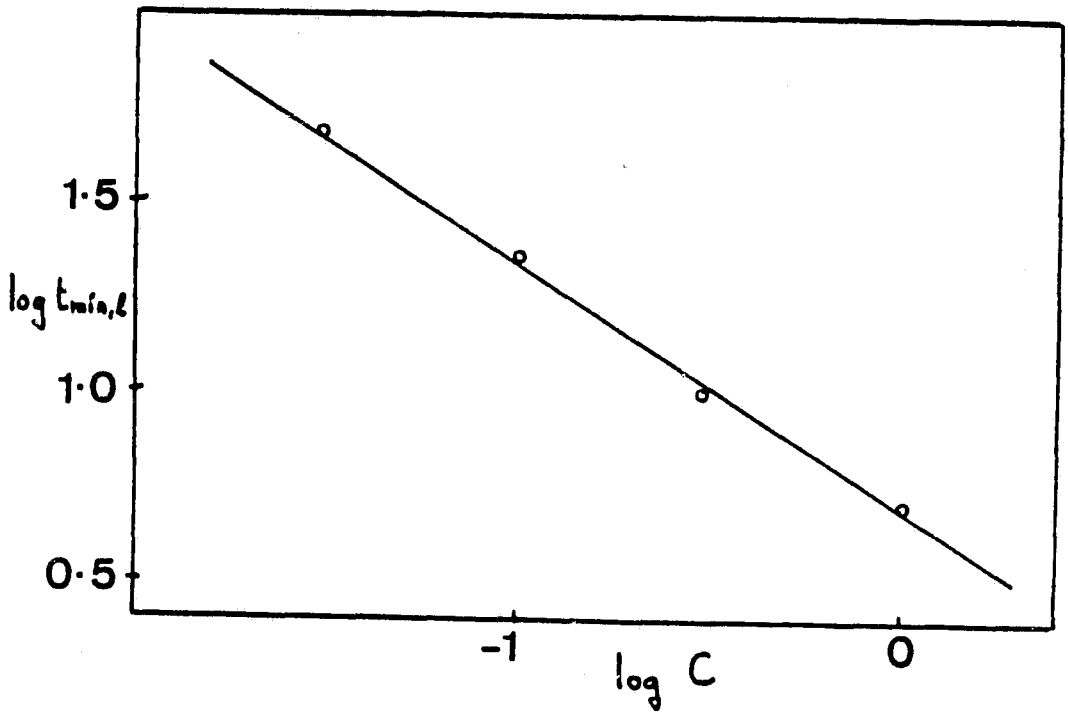

Figure 15 - Initiation time at the limiting current vs concentration in the TF configuration

$$t_{min,1_{(s)}} = 4.9\ C_{(M)}^{-2/3} \qquad \text{(III.5)}$$

The time scale of fluctuations Δt follows the same power law as a function of concentration and is typically half of $t_{min,1}$.

Again those findings are in agreement with WRAGG's results. Written in dimensionless quantities, (III.5) becomes :

$$\frac{Dt_{m,1}}{d^2} = 38\ Ra^{-2/3} \qquad \text{(III.6)}$$

where d is the electrode diameter. For WRAGG[43] the coefficient in (III.6) is 32.5 instead of 38 but this can be still considered a very good agree - ment. Relation (III.6) means that $t_{min,1}$ also is independent of electrode dimensions (as it is expected for a turbulent flow).

The boundary layer thickness (BLT) in pure diffusion is given by :

$$\delta = 2.77\ \sqrt{Dt} \qquad \text{(III.7)}$$

(here the BLT is defined as the distance at which $c = .95\ C_{bulk}$)
Using this relation and taking δ_m (value of δ at $t_{min,1}$) as a characteristic dimension one can derive a critical value of the Rayleigh number below which convection cannot take place :

$$Ra_{Cr} = \frac{g\gamma\ \delta_m^3\ C_{bulk}}{\nu D} \qquad \text{(III.8)}$$

Indeed, combining (III.5, 7, 8) one finds :

$$Ra_{Cr} \simeq 5000$$

This is substantially higher than the value given by SPARROW et al[47] (1800) or WRAGG (2400).

Finally, fig. 16 shows the evolution of the flow pattern as convection starts developping. The minimum in the I-t curve is when

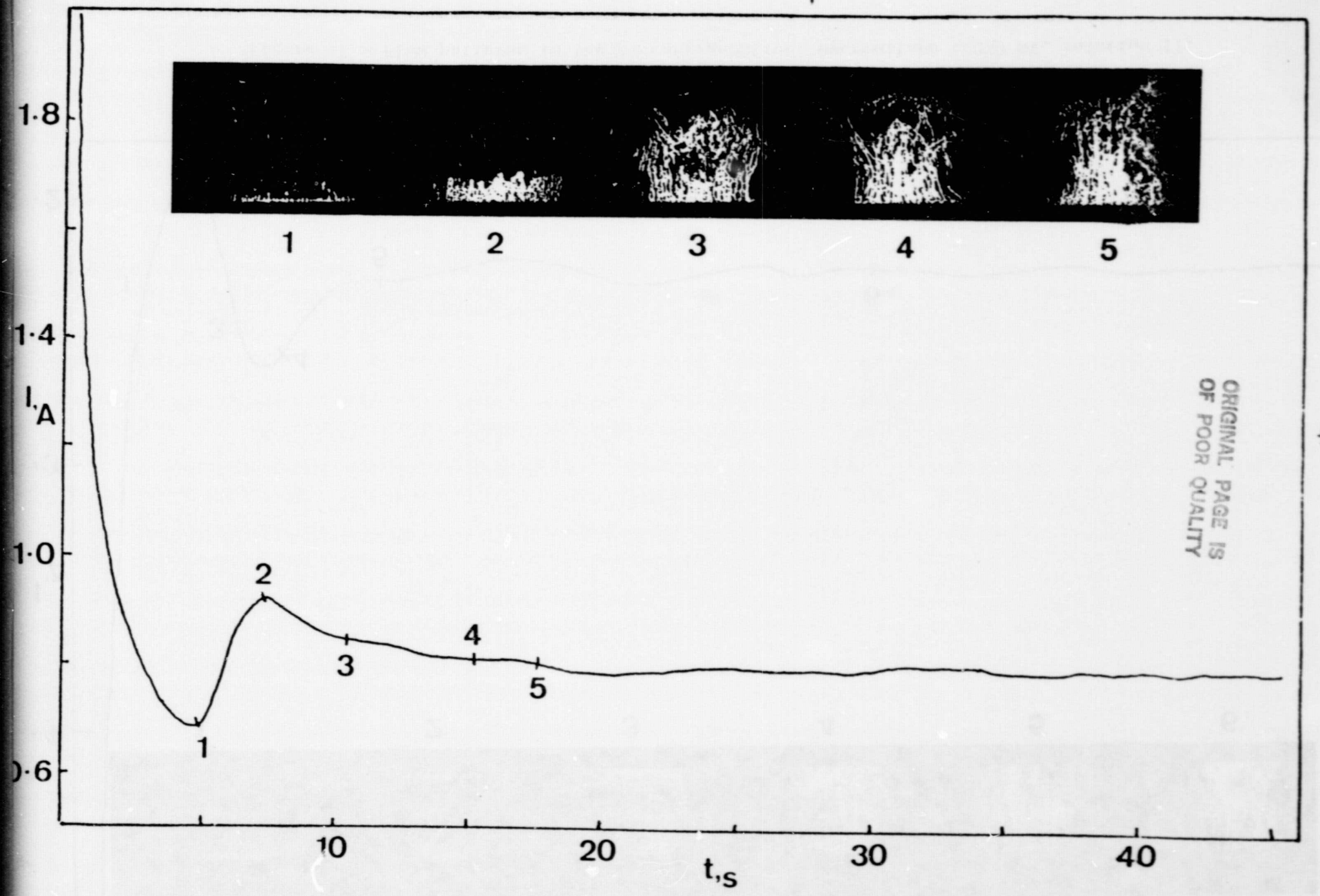

Figure 16 - Flow patterns in the TF configuration. Overvoltage : 250 mV, solution I.

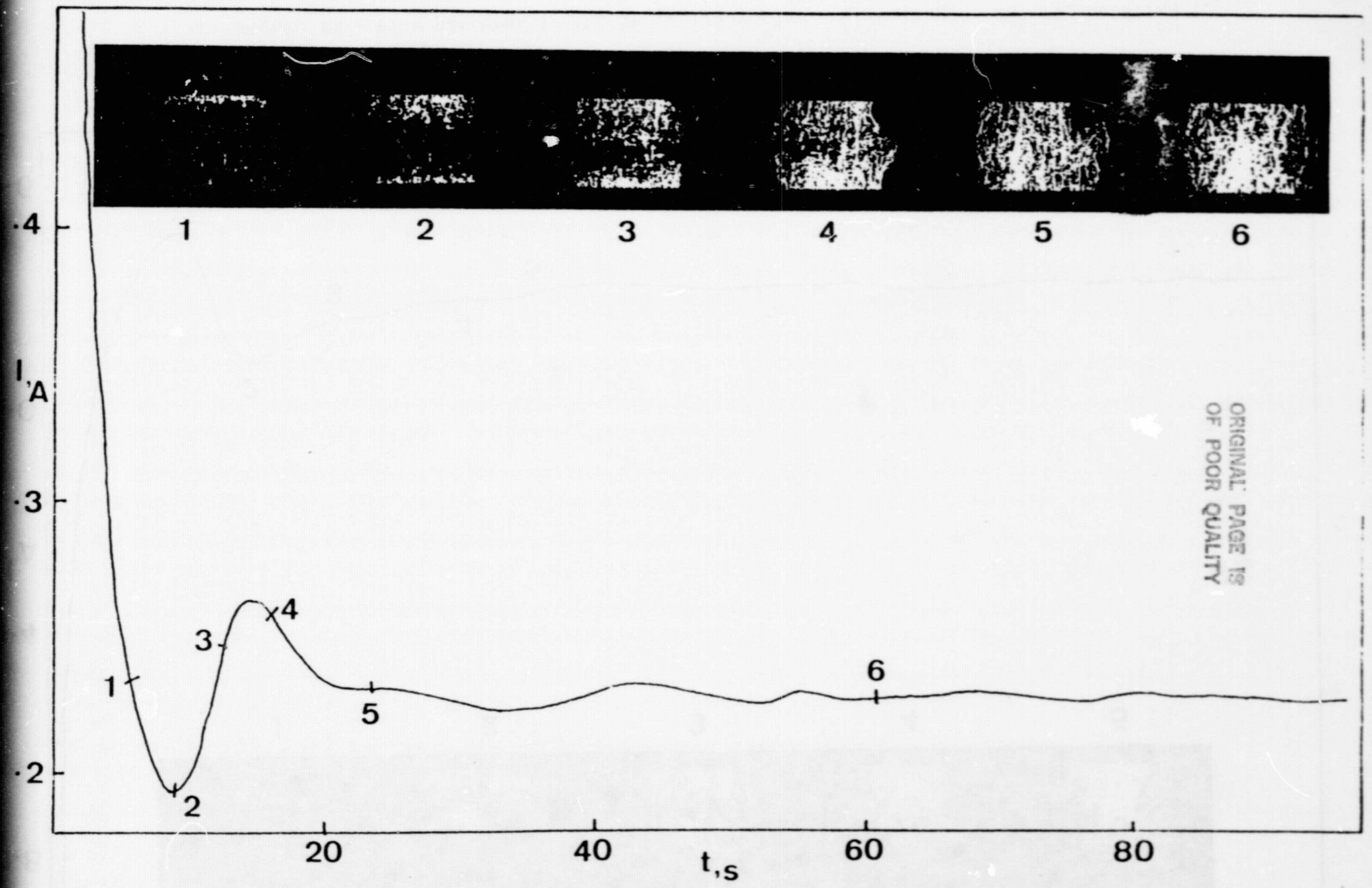

Figure 17 - Flow patterns in the AT configuration. Overvoltage : 250 mV, solution II.

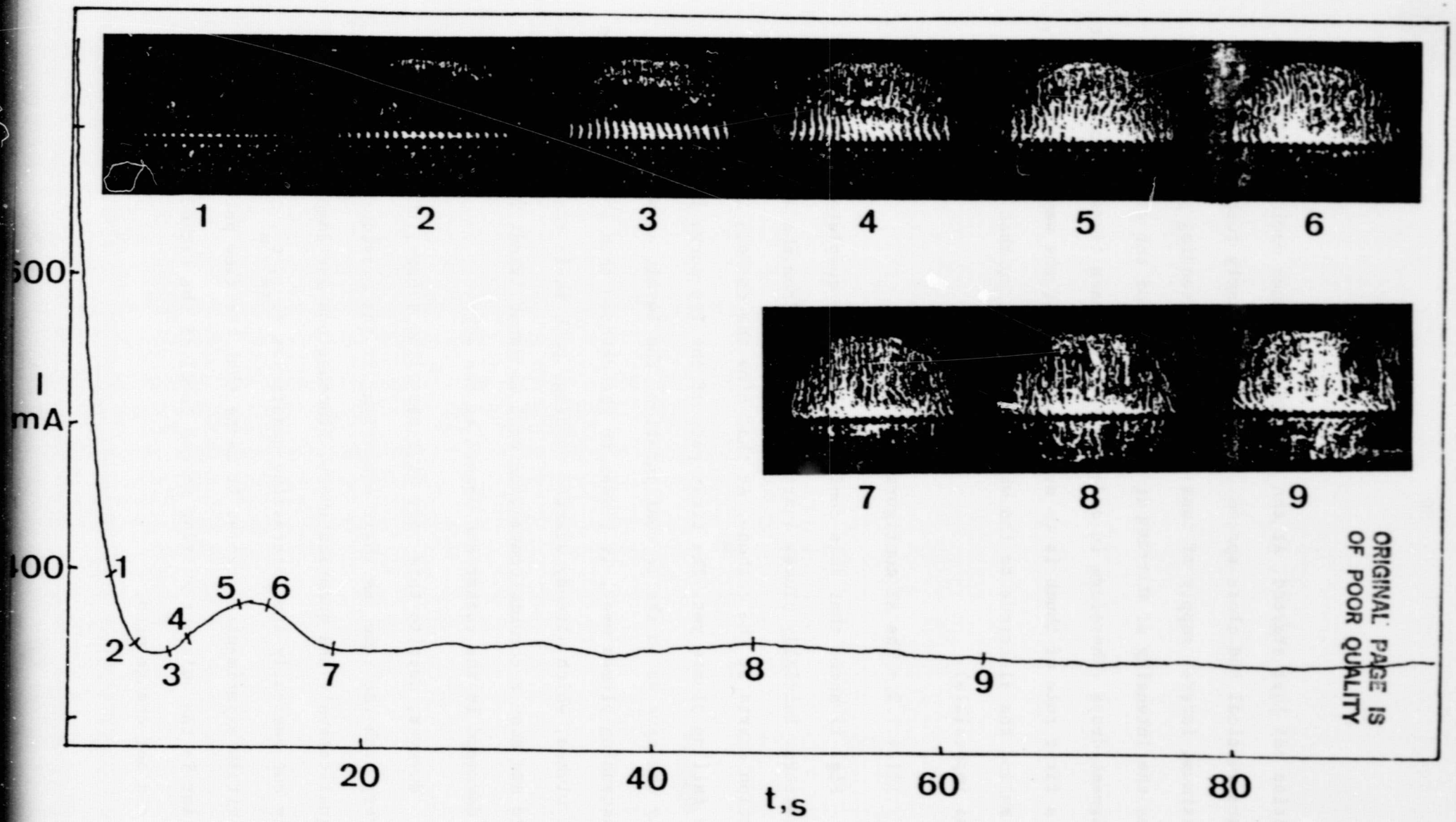

Figure 18 - Flow patterns in the G configuration. Overvoltage : 200 mV, solution II.

convection has just started. At the maximum the plumes coming off the surface are vertical and close spaced. The flow is clearly turbulent. After the maximum, lateral supply of ions squeezes the ascending plumes. Necking reduces the intensity of stirring at the outer edge of the electrode and the current drops (Therefore in order to keep the mass transfer coefficient high, a first rule of thumb is to avoid necking. And the way to achieve it, is to extend the electrode to the walls of the cell so that lateral supply becomes impossible).

III.4.1.2 - The AT configuration

Fig. 17 shows that this configuration has a completely different flow pattern. Initially plumes start falling down from the anode. Later on convection starts at the cathode. At that time the cathode is not "aware" of the falling plumes yet. The first part of the I-t curve is therefore exactly the same as in the TF configuration. The level, at which ascending and descending plumes meet, is closer to the cathode than to the anode. The anodic plumes, which already started necking, push their rising counterpart outward and soon a toroidal convection cell is established. The electrolyte flows downward in the center and upward at the edge.

However, despite this very different flow scheme, the I-t curves look very much the same as their equivalent in the previous configuration both qualitatively and quantitatively. Fluctuations may damp out less rapidly but basically the interesting quantities (i_{ss}, t_m, Δt) are identical within experimental errors. It means that the flow pattern was only different in the bulk but stirring at the level of the cathodic boundary layer did not change much.

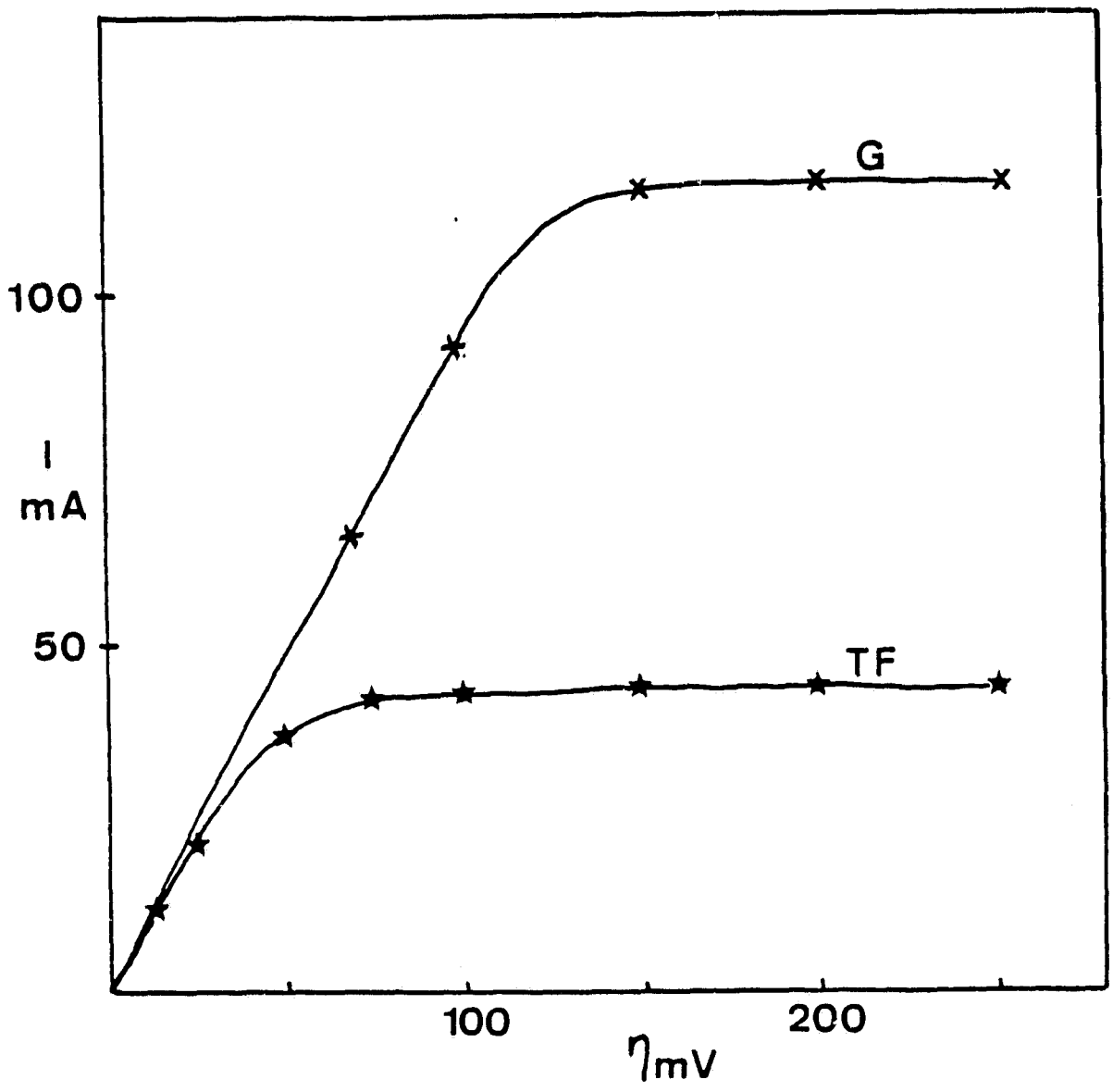

Figure 19 - I-V curves in the case of solution III with the TF and G configuration

III.4.1.3 - The G configuration

The evolution of the flow pattern (see fig. 18) is very similar to that in the previous case. However, now the falling plumes can go through the grid and the boundary layer around the wires of the grid is much more perturbed.

Although the I-t curves still look the same as the previous ones, there are significant quantitative differences. Fig. 19 compares the current-overpotential curves of solution III (0.1 M $ZnCl_2$) for the TF and G configuration. Although the absolute value of currents cannot be compared because of different electrode areas, we see that the limiting current is not reached until much higher overvoltages : assuming a linear relationship between i_{ss} and η, the limiting current would have been doubled.

III.4.2 - Long time deposition

A few long runs were carried out to study the effect of convection on long time deposition.

In the TF configuration, no useful information could be obtained because of gradual depletion of the solution. Indeed, with this arrangement, the catholyte and anolyte are practically separated. As deposition proceeds, the electrolyte above the cathode is poorer and poorer in solute whereas it becomes richer and richer below the anode.

Fig. 20 shows a chronogalvanometric recording of deposition from solution II in the AT configuration at 200 mV. The induction time, t_i, as defined earlier is found to be = 26 mn . If a vertical Pt wire was used as in Part II, it was estimated that t_i would have been around 7 mn.

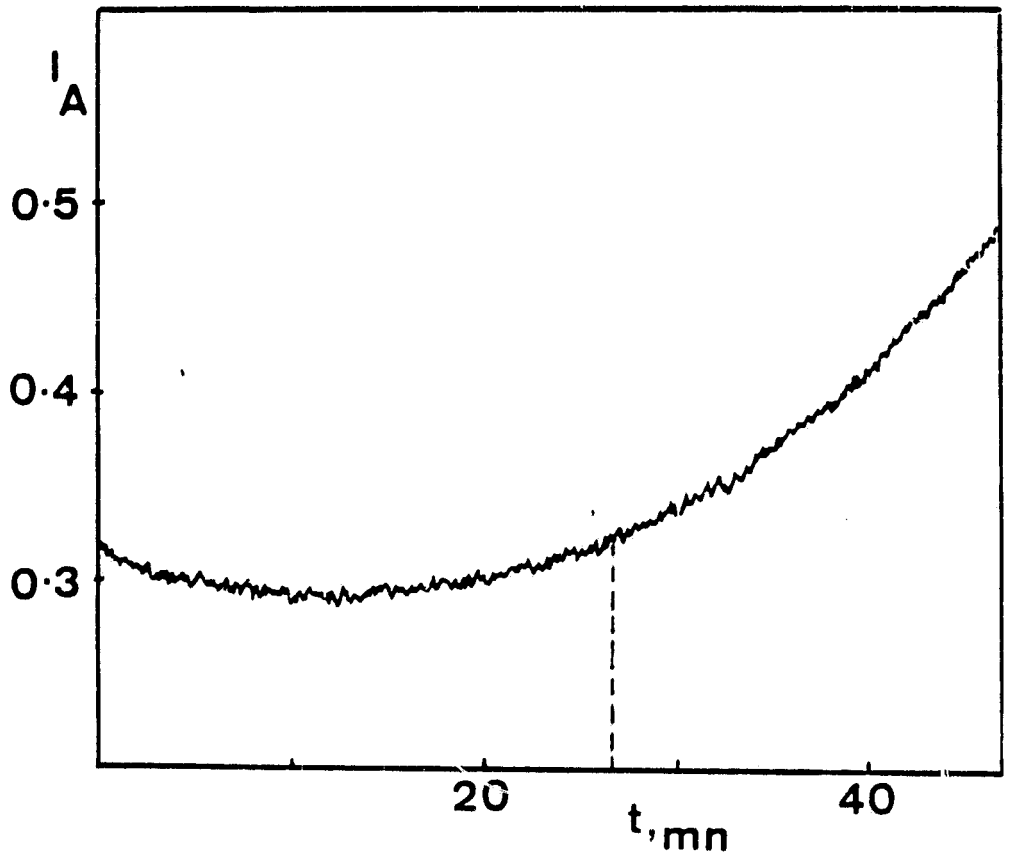

Figure 20 - Long time deposition in the AT configuration.

Solution II ; overvoltage = 200 mV.

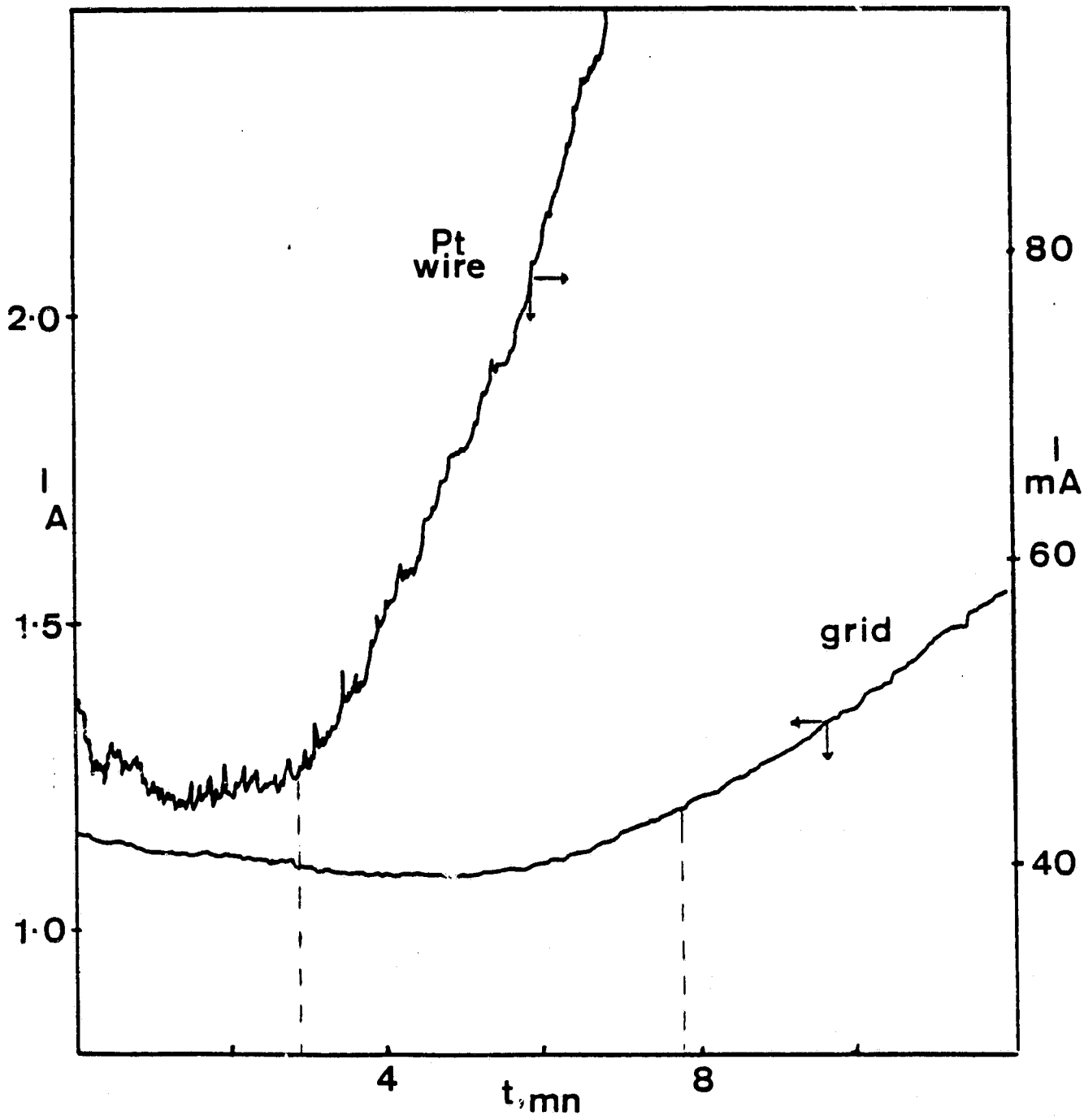

Figure 21 - Long time deposition on a Pt wire and on a horizontal grid (G configuration). Solution I ; overvoltage = 200 mV.

(From extrapolation of data on solutions I and III). This represents almost a four fold increase in time of sound deposition.

Fig. 21 compares results of deposition on the grid (the G configuration) and on the Pt wire previously studied (see Part II). Solution I was used, the overpotential was 200 mV. Induction times were respectively 7.6 mn and 3 mn. The other remarkable difference is the amplitude of fluctuations on both curves due to hydrogen evolution. Clearly the latter was much more effectively inhibited with the horizontal grid geometry.

CONCLUSION

Zinc was electrodeposited from acid chloride baths. It was shown that :

- The knowledge of bath chemistry was a determining factor for any further investigation.

- The critical overpotential, η_c, for dentrite growth of zinc was 65 mV. Different values are reported in the litterature, where zinc was deposited from other types of solutions. This supports the kinematic interpretation of the critical overpotential put forward by DESPIC : η_c would be related to the exchange current density which in turn depends on the nature of the bath.

On the other hand, the interaction of convection, current and concentration was studied below and at the limiting current. In-situ observation of flow patterns was possible through a laser schlieren visualization technique. Convection is extremely geometry sensitive and was studied for three configurations of horizontal electrodes (fig. 8).

In the top free configuration, the unperturbed convective flow above a horizontal upward facing cathode was investigated. Correlations of current and initiation time with concentration were in agreement with results in the litterature. They indicated that the Rayleigh numbers involved were high enough so that convection is turbulent and independent of electrode dimensions. To the contrary of what was published so far, current-voltage curves exhibited a well defined plateau suggesting that hydrogen evolution has been considerably reduced. A critical Rayleigh number for the onset of convection was found to be around 5000. This value is substantially higher than those

given by SPARROW or WRAGG. Putting the anode on the top of the cathode enabled long time deposition. The flow pattern in the bulk was very different from the previous configuration but the electrochemical performances were practically unchanged. However the use of a cathode grid doubled the limiting current. In both cases, sound deposits were obtained for times at least twice as long as with a vertical Pt wire.

Those encouraging results are worth extending to molten salt cells. A special furnace allowing laser schlieren observations in this case has been already built. However a significant improvement in controlling deposit morphology will not be possible as long as we lack a good theory of surface instabilities during electrocrystallization.

Laser schlieren is a very useful qualitative technique to observe macroscopic flow but is inappropriate to study fluid flow within the boundary layer. What one really needs is precisely a probe, a sort of a laser schlieren microscope, that can go down to the submillimeter level, determine concentration and velocity profiles ahead of the electrode surface and help understanding how and why surface roughening occurs.

APPENDIX I

Abundance of Zinc complexes in $ZnCl_2$ aqueous solutions

For a binary electrolyte of molar concentration C, the general decomposition reaction is :

$$C\ ZnCl_2 \rightarrow x\ Zn^{2+} + y\ ZnCl^{+} + z\ ZnCl_2 + t\ ZnCl_4^{2-} + u\ Cl^{-}$$

Five equations are needed to determine x, y, z, t and u :

$$\begin{cases} \text{conservation of zinc :} & x + y + z + t = C & (1) \\ \text{charge neutrality :} & 2x + y - 2t - u = 0 & (2) \\ \text{equilibrium 1} \quad (ZnCl^{+} \rightleftarrows Zn^{2+} + Cl^{-}) : & \dfrac{xu}{y} = k & (3) \\ \text{equilibrium 2} \quad (ZnCl_2 \rightleftarrows Zn^{2+} + 2Cl^{-}) : & \dfrac{xu^2}{z} = K_1 & (4) \\ \text{equilibrium 3} \quad (ZnCl_4^{2-} \rightleftarrows ZnCl_2 + 2Cl^{-}) : & \dfrac{zu^2}{t} = K_2 & (5) \end{cases}$$

k, K_1, K_2 are the pseudo-dissociation constants. They are concentration dependent and they are related to the true dissociation constants $\hat{k}$, $\hat{K}_1$, $\hat{K}_2$ through the mean activity coefficient $\gamma_{\pm}$. For instance :

$$\hat{k} = \frac{a_{Zn^{2+}} \cdot a_{Cl^{-}}}{a_{ZnCl^{+}}} = \frac{(\gamma_{\pm} x) \times (\gamma_{\pm} u)}{\gamma_{\pm}\ y} = \gamma_{\pm}\ k$$

Similarly $\hat{K}_1 = \gamma_{\pm}^2\ K_1$ and $\hat{K}_2 = \gamma_{\pm}^2\ K_2$

from (3) : $y = x \dfrac{u}{k}$ (3')

from (4) : $z = x \dfrac{u^2}{K_1}$ (4')

from (4') & (5) : $t = x \dfrac{u^4}{K_1 K_2}$ (5')

Replacing y, z and t by their values in (1), one gets :

$$x + x\frac{u}{k} + x\frac{u^2}{K_1} + x\frac{u^4}{K_1K_2} = C$$

$$\Rightarrow \quad X = \frac{C}{x} = 1 + \frac{u}{k} + \frac{u^2}{K_1} + \frac{u^4}{K_1K_2}$$

let $U = \frac{u}{k}$ (6) , then

$$X = 1 + U + \frac{k^2}{K_1}U^2 + \frac{k^4}{K_1K_2}U^4$$

$$X = 1 + U + \frac{\hat{k}^2}{\hat{K}_1}U^2 + \frac{\hat{k}^4}{\hat{K}_1\hat{K}_2}U^4 \qquad (7)$$

Hence, percentage of Zn^{2+} $= \frac{x}{C} = \frac{1}{X}$ (8)

percentage of $ZnCl^{+}$ $= \frac{y}{C} = \frac{U}{X}$ (9)

percentage of $ZnCl_2$ $= \frac{z}{C} = \frac{\hat{k}^2}{\hat{K}_1}\frac{U^2}{X}$ (10)

percentage of $ZnCl_4^{2-}$ $= \frac{t}{C} = \frac{\hat{k}^4}{K_1K_2}\frac{U^4}{X}$ (11)

Finally, replacing x, y and t by their value (eq. 8, 9, 11) in (2) leads to :

$$C = \frac{k\ X\ U}{2+U-\frac{\hat{k}^4}{\hat{K}_1\hat{K}_2}U^4} = \frac{1}{\gamma \pm} B \qquad (12)$$

where

$$B = \frac{\hat{k}\ X\ U}{2+U-\frac{\hat{k}^4}{\hat{K}_1\hat{K}_2}U^4} \qquad (13)$$

For each value of U, the percentage of each species present in the solution as well as the value of B can be calculated. U reaches a limiting value as B becomes infinite. The concentration C is found by solving each time : $C \cdot \gamma_{\pm}(C) = B$

Knowing C and B, one can deduce their ratio $\gamma_{\pm}$ and get the last quantity u from (6) :

$$u = kU = \frac{\hat{k}\, U}{\gamma_{\pm}}$$

Data concerning mean activity coefficient were available in the litterature[56]. $\gamma_{\pm}$ vs concentration was well correlated by :

$$\gamma_{\pm} = \frac{1.0 - .55 \log C}{3} \qquad (14)$$

in the range 10^{-3} - 1M

$\hat{k}$ was obtain from Ref. 6 : $\hat{k} = .22$

whereas K_1 and K_2 were given for concentrations around 2 M in Ref. 8 :

$$K_1 = 3.15 \times 10^{-2}\ M^2$$

$$K_2 = 4 \times 10^{-2}\ M^2$$

using (13) one gets : $\hat{K}_1 = 2.4 \times 10^{-3}$

$$\hat{K}_2 = 3.1 \times 10^{-3}$$

Addition of a supporting electrolyte

From fig. 1, it is clear that over the whole range of usual concentrations, there is no dominant ionic species. However one can displace equilibria 1 to 3 towards the fully complexed state $ZnCl_4^{2-}$ by adding an inert chloride salt. Let A be the concentration of this new salt, say NaCl.

The only equation altered by this addition is that of charge neutrality. It becomes :

$$A + 2x + y - 2t - u = 0 \qquad (2')$$

where the concentration of chloride ions is now a free parameter.

Comparing (11) and (10) one finds that $z > 10t$ if :

$$\frac{\tilde{k}^4}{\tilde{K}_1 \tilde{K}_2} U^4 > 10 \frac{\hat{k}^2}{\hat{K}_1} U^2$$

$$\Leftrightarrow \quad U^2 > 10 \frac{\hat{K}_2}{\hat{k}^2} \quad \Leftrightarrow \quad (u \cdot \gamma_{\pm})^2 > 10 \hat{K}_2$$

$$\Leftrightarrow \quad u > .5 \text{ M} \quad \text{for } \gamma_{\pm} \simeq .3$$

on the other hand : $u > \underbrace{A - 2C}_{u_{min}}$

minimum value in case all zinc was converted into $ZnCl_4^{2-}$

Therefore, zinc could be considered fully complexed as long as :

$$A - 2C > .5 \text{ M}$$

APPENDIX II

Curve fitting procedure for the determination of the critical overpotential

After POPOV[33], dentrites initially grow at an exponential rate. Correspondingly, the cathode area and therefore the total current increases at the same rate. Thus the current can be written as :

$$I(t) = I_o + A \exp \frac{t}{\tau}$$

I_o is the steady state current associated with a planar front deposition, A is a constant and τ is the time constant of surface roughening.

Below a critical overpotential dentrites cannot form and gradual amplification of initial asperities has a time constant independent of overpotential. Above the critical overpotential dentrites grow at a rate proportional to the square of overpotential.

The problem in estimating τ is that I_o is not known and taking the minimum value for I_o does not lead to a good fit. A way to circumvent the problem is to fit the derivative of I to an exponential and not I itself :

$$\frac{dI}{dt} = \frac{A}{\tau} \exp (t/\tau) = B \exp (t/\tau)$$

This is precisely what was done : $\frac{dI}{dt}$ was approximated by $\frac{I(t_n) - I(t_{n-1})}{t_n - t_{n-1}}$.

A linear regression of $\log \frac{dI}{dt}$ vs t gave a value of τ. This value was checked by another linear regression of I vs $\exp (\frac{t}{\tau})$. The high values of the correlation coefficient (> 80 % in the first case and > 97 % in the second) confirmed the validity of the procedure.

BIBLIOGRAPHY

1. L.S. LILICH, Y.S. VARSHAVSKY, Russian J. Gen. Chem., 26 (1956), 337-341

2. J. BESSON, W. ECKERT, Bull. Soc. Chim. (1959), 1676-1681

3. G. SCHORSCH, Soc. Chim. Fran., Mémoires 1964, 1449-1455

4. A. AGNEW, R. PATTERSON, J.C.S. Faraday I, 74 (1978), 2896-2906

5. R. PATTERSON, Faraday Disc. Chem. Soc., 64 (1977), 304-321

6. LUTFALLAH et al., J.C.S. Faraday I, 72 (1976), 495

7. Handbook of Chem. and Phys., CRC Press 1981-1982

8. B. GILBERT, Bull. Soc. Chim. Belges, 76 (1967), 493-504

9. D.E. IRISH et al., J. Chem. Phy., 39 (1963), 3436-3444

10. W. LORENZ, Z. Phy. Chem. N.F., 19 (1959), 377

11. L. GAISER, K.E. HEUSLER, Electrochi. Acta, 15 (1970), 161

12. H.B. SIERRA ALCAZAR, J.A. HARRISON, Ibidem, 22 (1977à, 627

13. J.T. KIM, J. JORNE, J. Electrochem. Soc, 127 (1980), 8-15

14. J.A. von WEBER, P. TOMASSI, Metalloberfläche, 31 (1977), 259

15. I. EPELBOIN et al, J. Electrochem. Soc, 122 (1975), 1206-1214

16. " Faraday Symp. Chem. Soc., 12 (1977), 115

17. " Electroanaly. Chem. and Inter. Electrochem., 58 (1975), 433-437

18. " J. Electroana. Chem., 65 (1975), 373-389

19. J. O'M. BOCKRIS et al, J. Electrochem. Soc., 119 (1972), 285

20. N.A. HAMPSON et al, J. Electroana. Chem., 25 (1970), 9

21. D.A. PAYNE, A.J. BARD, J. Electrochem. Soc., 119 (1972), 1113

22. V.N. TIMOVA, A.T. VAGRAMYAN, Electrokhimia, 2 (1966), 1149
" " Za. Sch. Metallov., 3 (1967), 102

23. CHIN, VENKATESH, J. Electrochem. Soc., 128 (1981), 1434

24. Ph. BROUILLET, F. JOLAS, Electrochim. Acta, 6 (1962), 245

25. J.L. BARTON, J. O'M. BOCKRIS, Proc. Royal Soc., A 268 (1962, 485-505

26. A.R. DESPIC, K.I. POPOV, Modern Aspects of Electrochemistry, vol. 7, chap. 4, B.E. Conway, J.O'M Bockris Editors, Plenum Press, New York (1972)

27. N. IBL, Ph. JAVET, F. STAHEL, Electrochim. Acta, 17 (1972), 733-739

28. R. AOGAKI et al, Ibidem, 25 (1980), 965-972

29. W.W. MULLINS, R.F. SEKERKA, J. App. Phys., 34 (1963), 323

30. J.W. DIGGLE, A.R. DESPIC, J.O'M. BOCKRIS, J. Electrochem. Soc., 116 (1969), 1503-1514

31. S. TAJIMA, M. OGATA, Electrochim. Acta, 13 (1968), 1845
Ibidem, 15 (1970), 61

32. A.R. DESPIC; M.M. PURENOVIC, J. Electrochem. Soc., 121 (1974), 329-335

33. K.I. POPOV et al, J. Applied Electrochem., 9 (1979), 533-536

34. J.R. SELMAN, C.W. TOBIAS, Advanees in Chemical Engineering (1972)

35. J.N. AGAR, Disc. Faraday Soc., 1 (1947), 26-37

36. C. WAGNER, Trans. Electrochem. Soc., 95 (1949), 161

37. " J. Electrochem. Soc., 104 (1957), 129-131

38. C.R. WILKE et al, J. Electro. Soc., 100 (1953), 513-523

39. " Chem. Eng. Pro., 49 (1953), 663-674

40. N. IBL, R.H. MULLER, J. Elec. Soc., 105 (1958), 346

41. N. IBL, CITCE Proc. of 8th Meeting (1958), 174-189

42. A.A. WRAGG, Electrochim. Acta, 13 (1968), 2159-2165

43. M.A. PATRICK, A.A. WRAGG, Int. J. Heat Mass Transfer., 18 (1975) 1397-1407

44. A.A. WRAGG, R.P. LOOMBA, Ibidem, 13 (1970), 439-442

45. M.A. PATRICK et al, The Can. J. of Chem. Eng., 55 (1977), 432-438

46. A.A. WRAGG, A.K. NASRUDDIN, Electrochim. Acta 18 (1973), 619-627

47. J.R. LLOYD, E.M. SPARROW, J. Fluid Mech., 42 (1970), 564

48. J.R. SELMAN, J. TAVAKOLI-ATTAR, J. Elect. Soc., 127 (1980), 1049-1055

49. L.A. VASILEV, Schlieren Methods, Keter Publishers Ltd, London (1971)

50 G. WRANGLEN, Acta Chem. Scand., 12 (1958), 1543-1544

51. STEPHENSON, BARLETT, J. Electrochem. Soc., 101 (1954), 571

52. N. IBL, CITCE Proc. 7th Meeting (1955), 112

53. R.B. OWEN, Opti. Eng., 20 (1981) 634-638

54. R.B. OWEN, M.H. JOHNSTON, Optics and Lasers in Eng., 2 (1981), 129-146

55. P.S. CHEN et al, Crystal Growth, 47 (1979), 43-60

56. G.V. AKIMOV, Theory and experimental methods of metal corrosion, Leningrad-Moscou, Academy of Science

BIOGRAPHY

Mr ABDELMASSIH was born in [redacted] in [redacted]. He was first educated in Lebanon. He went afterwards to France where he pursued engineering studies. In 1980, he graduated from Ecole Nationale Supérieure des Mines de Paris.

His experience includes training periods at :

- A Pechiney / Rhône-Poulenc plant, Salindres, France (1978)
- The Central Electricity Research Laboratory, Leatherhead, U.K. (1979)
- IRSID, Saint Germain-en-laye, France (1980)